



# Exchange protein directly activated by cAMP (Epac) 1 plays an essential role in stress-induced exercise capacity by regulating PGC-1 $\alpha$ and fatty acid metabolism in skeletal muscle

Wai-Kin So<sup>3</sup> · Hyoung Kyu Kim<sup>2</sup> · Yingxian Chen<sup>3</sup> · Seung Hun Jeong<sup>2</sup> · Patrick Ka Kit Yeung<sup>3</sup> · Billy C. K. Chow<sup>5</sup> · Jin Han<sup>2</sup> · Sookja K. Chung<sup>1,3,4</sup>

Received: 11 November 2019 / Revised: 19 December 2019 / Accepted: 27 December 2019  
© Springer-Verlag GmbH Germany, part of Springer Nature 2020

## Abstract

Exchange protein directly activated by cAMP (Epac) mediates cAMP-mediated cell signal independent of protein kinase A (PKA). Mice lacking Epac1 displayed metabolic defect suggesting possible functional involvement of skeletal muscle and exercise capacity. Epac1 was highly expressed, but not Epac 2, in the extensor digitorum longus (EDL) and soleus muscles. The exercise significantly increased protein expression of Epac 1 in EDL and soleus muscle of wild-type (WT) mice. A global proteomics and pathway analyses revealed that Epac 1 deficiency mainly affected “the energy production and utilization” process in the skeletal muscle. We have tested their forced treadmill exercise tolerance. Epac1<sup>-/-</sup> mice exhibited significantly reduced exercise capacity in the forced treadmill exercise and lower number of type 1 fibers than WT mice. The basal protein level of proliferator-activated receptor gamma coactivator 1-alpha (PGC-1 $\alpha$ ) was reduced in the Epac1<sup>-/-</sup> mice. Furthermore, increasing expression of PGC-1 $\alpha$  by exercise was also significantly attenuated in the skeletal muscle of Epac1<sup>-/-</sup> mice. The expressions of downstream target genes of PGC-1 $\alpha$ , which involved in uptake and oxidation of fatty acids, ERR $\alpha$  and PPAR $\delta$ , and fatty acid content were lower in muscles of Epac1<sup>-/-</sup>, suggesting a role of Epac1 in forced treadmill exercise capacity by regulating PGC-1 $\alpha$  pathway and lipid metabolism in skeletal muscle. Taken together, Epac1 plays an important role in exercise capacity by regulating PGC-1 $\alpha$  and fatty acid metabolism in the skeletal muscle.

**Keywords** Exchange protein directly activated by cAMP (Epac) · Exercise capacity · PGC-1 $\alpha$  · Fatty acid metabolism · Skeletal muscle

This article is part of the special issue on *Exercise Physiology: future opportunities and challenges in Pflügers Archiv—European Journal of Physiology*

Wai-Kin So and Hyoung Kyu Kim contributed equally to this work.

**Electronic supplementary material** The online version of this article (<https://doi.org/10.1007/s00424-019-02344-6>) contains supplementary material, which is available to authorized users.

✉ Jin Han  
phyhan@inje.ac.kr

✉ Sookja K. Chung  
skchung@must.edu.mo

<sup>1</sup> Macau University of Science and Technology, Faculty of Medicine, Taipa, Macau

<sup>2</sup> National Research Laboratory for Mitochondrial Signaling, Department of Physiology, Department of Health Sciences and Technology, BK21 Project Team, College of Medicine, Cardiovascular and Metabolic Disease Center Inje University, Busan, South Korea

<sup>3</sup> School of Biomedical Sciences, Research Center of Heart, Brain, Hormone and Healthy Aging, Li Ka Shing Faculty of Medicine, The University of Hong Kong, Pok Fu Lam, Hong Kong

<sup>4</sup> United International College, Beijing Normal University-Hong Kong Baptist University, Zhuhai, China

<sup>5</sup> School of Biological Sciences, The University of Hong Kong, Pok Fu Lam, Hong Kong

## Introduction

Skeletal muscle is the largest organ in the body; it plays critical roles in physical activities, metabolism (glucose disposal and lipid catabolism) and is associated with some pathological conditions like muscular dystrophies and sarcopenia [8, 21, 26]. The ability of skeletal muscle to respond to enhanced energy demand in terms of efficient and timely balance between glucose and lipid utilization is a form of metabolic plasticity essential for survival [3, 11, 16, 26]. Conversely, metabolic inflexibility in skeletal muscle can cause exercise intolerance, organ dysfunction, and disease [11].

Skeletal muscle physiology is essentially regulated by G protein-coupled receptor (GPCR)-cAMP signaling [1, 9, 21], from the regulation of acute metabolic changes during exercise to the developmental and structural changes of skeletal muscle in the long term [5].  $\beta_2$ -adrenergic receptor ( $\beta_2$ -AR) is the prevalent  $\beta$ -AR on skeletal muscle and  $\beta_2$ -AR/cAMP represents one of the best-characterized GPCR/cAMP signaling pathways in skeletal muscle. During exercise, epinephrine, via  $\beta_2$ -AR, promotes acute changes in muscle contraction and energy utilization, such as faster excitation contraction coupling [35]. Chronic  $\beta_2$ -AR activation would lead to skeletal muscle hypertrophy with increased protein synthesis and reduced protein degradation.  $\beta_2$ -AR agonists have been used as ergogenic to boost athletic performance [21]. Clinically, pharmaceutical manipulation of cAMP signaling, such as by the use of  $\beta_2$ -AR agonists, has proven beneficial to people suffer from skeletal muscle disorders like sarcopenia, cancer cachexia, and muscular dystrophies [5].

Two cAMP sensors, protein kinase A (PKA) and exchange protein directly activated by cAMP (Epac), mediate cAMP responses. Despite the importance of the cAMP signaling in skeletal muscle, the molecular mechanisms mediating cAMP actions are still being elucidated. Particularly, most of the knowledge is restricted to the conventional cAMP effector protein kinase A (PKA) whereas information about the newly identified effector Epac is extremely limited.

The two Epac isoforms, Epac1 and Epac2, are guanine nucleotide exchange factors for the small G protein Rap [6]. Our laboratory has generated mice carrying homozygous deletion of Epac1 isoform and showed that Epac1<sup>-/-</sup> mice displayed metabolic phenotypes, including impaired glucose tolerance and lower glucose-stimulated insulin secretion [18]. Importantly, Epac1<sup>-/-</sup> mice exhibited significantly higher respiratory exchange ratio, elevated circulating triglyceride TG levels. The present work started with examining whether the perturbation of lipid metabolism would compromise physical exercise performance. The present work also demonstrated that, Epac1<sup>-/-</sup>, as well as Epac2<sup>-/-</sup> and Epac1<sup>-/-</sup>; Epac2<sup>-/-</sup> mice exhibited significantly reduced exercise capacity when compared with wild-type (Epac1<sup>+/+</sup>; Epac2<sup>+/+</sup>) mice. As muscle fiber composition and lipid utilization are critical

determinants of exercise capacity, to address the hypothesis that exercise intolerance in Epac-deficient mice could stem from defects in these aspects in skeletal muscle, immunocytochemical experiment showed that Epac knockout (KO) shifted the muscle fiber to fast-twitch type. Furthermore, fatty acid (FA) and triglyceride homeostasis were found perturbed in Epac KO muscle. Both resting and exercised Epac-deficient muscle contained reduced level of master transcription coactivator PGC-1A mRNA than the wild-type counterpart. The present study elucidates the role of Epac1 in skeletal muscle fiber typing, lipid utilization, and physical exercise performance.

## Materials and methods

### Animal experiments

All animal experiments were conducted following the guidelines approved by Committee on the Use of Live Animals in Teaching and Research of The University of Hong Kong (CULATR 3175-13) and Inje University Animal Care and Use Committee (IACUC 2014-037). Mice were housed with a 12-h light/dark cycle (L 0700 to 1900 h) and ad libitum access to food and water. All the mouse lines used in the present study were obtained and bred according to the previously published paper [37]. Eight- to 12-week male WT, Epac1<sup>-/-</sup>, Epac2<sup>-/-</sup> and Epac1<sup>-/-</sup>; 2<sup>-/-</sup> mice were used in all experiments, unless otherwise stated.

### Graded treadmill running test

Treadmill running test was conducted according to the published protocols [13, 22]. Mice were trained for 3 days with running on the treadmill with 5° inclination at 10 cm/s for 5 min and 15 cm/s for 10 min. The treadmill was equipped with an electric shock apparatus to keep the mice running. On the testing day, mice were allowed to run on the treadmill with 10° inclination at 10 cm/s for 5 min and 15 cm/s for 10 min and the speed was increased by 3 cm/s every 2 min. The mice were allowed to run until exhaustion when the mice unable to run on the treadmill for 10 s despite mechanical prodding. Body weight, weight of tissues, running time, running distance, number, and duration of electric shocks were measured. Work done performed was calculated using the published formula [29]: body weight (kg) × running distance (m) × Sin (slope degree) × 9.8 (J/kg × m).

### One-dimensional LC-MS/MS proteome analysis

Protein separation and LC-MS analysis were performed as previously described [19]. Briefly, dissolved skeletal soleus muscle proteins from wild-type, Epac1<sup>-/-</sup>, Epac2<sup>-/-</sup> and

Epac1<sup>-/-</sup>; Epac2<sup>-/-</sup> mice were separated on a 12% polyacrylamide gel by SDS-PAGE. The gels were washed three times with ddH<sub>2</sub>O for 5 min each and then stained with Bio-Safe Coomassie stain solution (Coomassie G250 stain; Bio-Rad, Hercules, CA) for 1 h, with gentle shaking at room temperature. The Coomassie-stained gels were evenly sliced into 10 slices and then destained by incubation in 75 mM ammonium bicarbonate/40% ethanol (1:1). Disulfides were reduced by treatment with 5 mM DTT/25 mM ammonium bicarbonate at 60 °C for 30 min, followed by alkylation with 55 mM iodoacetamide at room temperature for 30 min. The gel pieces were then dehydrated in 100% acetonitrile (ACN), dried, and swollen overnight at 37 °C in 10 μl 25 mM ammonium bicarbonate buffer containing 20 μg modified sequencing grade trypsin (Roche Applied Science, Indianapolis, IN)/ml. The tryptic peptide mixture was eluted from the gel with 0.1% formic acid. LC-MS/MS analysis was performed using a ThermoFinnigan ProteomeX workstation LTQ linear ion trap MS (Thermo Electron, San Jose, CA) equipped with NSI sources (Thermo Electron). Briefly, 12 μl of peptide sample from the in-gel digestion was injected and loaded onto a peptide trap cartridge (Agilent, Palo Alto, CA). Trapped peptides were eluted onto a 10-cm reversed phase (RP) PicoFrit column packed in-house with 5-μm 300-Å pore size C18, then separated by gradient elution. The mobile phases consisted of H<sub>2</sub>O and ACN, both containing 0.1% v/v formic acid. The flow rate was maintained at 200 nl/min. The gradient started at 2% ACN, then reached 60% ACN in 50 min, 80% ACN in the next 5 min, and 100% H<sub>2</sub>O in the final 15 min. Data-dependent acquisition (*m/z* 400–1800) was enabled, and each MS survey scan was followed by five MS/MS scans within 30 s, with the dynamic exclusion option enabled. The spray voltage was 1.9 kV, the temperature of the ion transfer tube 195 °C, and the normalized collision energy was 35% [27].

Data-analyzed tandem mass spectra were extracted and the charge state deconvoluted and de-isotoped using the Sorcerer 3.4 beta2 platform (Sorcerer software 3.1.4, Sorcerer Web interface 2.2.0 r334, and Trans-, Proteomic Pipeline 2.9.5). All MS/MS samples were analyzed using SEQUEST (version v.27, rev. 11; ThermoFinnigan, San Jose, CA), which was set to search the ipi 3.29 database (IPI ver.3.29, 40131 entries) with semitrypsin as the digestion enzyme. The search used a fragment-ion mass tolerance of 1.00 Da and a parent-ion mass tolerance of 1.5 Da. Iodoacetamide-derivatized cysteine was specified as a fixed modification. Methionine oxidation, iodoacetamide derivatization of cysteine, and phosphorylation of serine, threonine, and tyrosine were specified as variable modifications. Scaffold (version Scaffold-2.0; Proteome Software Inc., Portland, OR) was used to validate MS/MS-based peptide and protein identifications. Peptide identifications were accepted if their probability was >95.0%, as specified by the Peptide Prophet algorithm, and they contained at least one identified peptide. Protein probabilities were

assigned by the Protein Prophet algorithm. Proteins containing similar peptides such that they could not be differentiated based on MS/MS analysis alone were grouped to satisfy the principles of parsimony. After identifying the proteins, each dataset was used for a subtractive analysis by semi-quantitative normalized spectral counts, which were normalized by total spectral counts in the Scaffold program [24].

### Bioinformatics analysis

In order to elucidate the molecular functions and biological processes of the identified proteins, the proteins were further categorized and annotated, and functional networks were constructed. Systematic bioinformatics analysis of the proteome was conducted using STRING 10.0 (Search Tool for the Retrieval of Interacting Genes/Proteins) [34] and Ingenuity Pathway Analysis Software (IPA, <http://www.ingenuity.com>) [20].

### Real-time PCR

Total RNA was extracted from tissues using TRIzol Reagent (Invitrogen) and used in first-strand DNA (cDNA) synthesis using the PrimeScript RT Master Mix (Takara, Japan) for real-time PCR according to the manufacturer's protocol. Real-time PCR was performed in Bio-Rad iQ5 real-time thermal cycler (Bio-Rad, Hercules, CA). Primer sequences are available upon request. The amplifications of target genes the internal control GAPDH were performed as follows: a 3-min hot start at 95 °C followed by 40 cycles of denaturation at 95 °C for 15 s and amplification at 60 °C for 30 s.

### Western blot analysis

Equal amounts of total cell lysate were resolved on 7.5–15% SDS-PAGE gels and electrotransferred to a PVDF membrane. After blocking for 1 h with 5% nonfat dry milk in TBS-T buffer (20 mM Tris-HCl, pH 7.4, 150 mM NaCl, 0.1% Tween-20), the blots were probed for overnight at 4 °C with the following primary antibodies: anti-Epac1 (kindly provided by Professor J. Bos from the UMC Utrecht), anti-PKA regulatory subunit 1 alpha (Abcam, Cambridge, MA), anti-GLUT4 (provided by Dr. Aimin Xu, The University of Hong Kong), anti-phospho-CREB, anti-phospho-AKT (Ser473), anti-phospho-AMPKa (Thr172) (Cell Signaling, Inc., Austin, TX), anti-SIRT1 (Santa Cruz Biotechnology, Inc., Santa Cruz, CA), anti-tubulin antibody (Sigma, St. Louis, MO). Anti-VDAC, anti-NDUFS4, anti-CX II 70kD FP, anti-CX III subunit core 2, anti-COX-IV and were gifts from Dr. Philip Ho, The University of Hong Kong. The blots were then incubated with a peroxidase-conjugated secondary antibody (Bio-Rad) for 1 h followed by detection with ECL chemiluminescence reagent (Amersham, Arlington Heights, IL) and exposure on X-ray films.

## Immunocytochemistry

Gastrocnemius were fixed in 4% paraformaldehyde for around 48 h and embedded in paraffin for sectioning. Five- $\mu\text{m}$  sections were prepared using microtome and mounted on pre-coated microscopic slides. Immunostaining with anti-type I myosin heavy chain antibody (1:1000) was performed on the sections using a Vectastain Elite ABC kit. The sections were counter-stained with hematoxylin before mounting. Images were captured with a Spot RT Color CCD digital camera connected to an inverted microscope. Cross-section area of positively stained fiber was quantified by ImageJ software.

## Mitochondrial DNA quantification

Total DNA was extracted from muscles using TRIzol Reagent. Real-time PCR was performed using primers specific for the mouse mitochondrial genes COX-II and ND-1 and mitochondrial DNA content were normalized against DNA content of nuclear gene,  $\beta$ -globin (Primer sequences are available upon request).

## Isolation and culture of primary satellite cells

The soleus and gastrocnemius were dissected from wild-type mice. Tendon, fat, vessel, and connective tissues were carefully removed under a dissecting microscope. Muscles were cut into small pieces and incubated with 0.1% collagenase H at 37 °C for 1 h. After digestion, the slurry was centrifuged at 400g for 15 min. The pellet was resuspended in growth medium (DMEM with 20% FBS and 2.5 ng/mL recombinant human FGF) and triturate using pipette to dislodge satellite cells from muscle fibers. The mixture was filtered through a 40- $\mu\text{m}$  nylon mesh rinsed with proliferation medium. The cell suspension was pelleted by centrifugation at 1000g for 10 min. The pellets containing satellite cells were resuspended in proliferation medium and plated on matrigel-coated culture dishes. Primary satellite cells were cultured in growth medium until become confluent. Culture medium was then replaced with differentiation medium (DM, DMEM with 2% horse serum and 5  $\mu\text{g/ml}$  insulin) and maintained in 5%  $\text{CO}_2$  at 37 °C for 7 days. Differentiation medium was changed every 2 days. Myotubes differentiated from wild-type satellite cells were incubated with 0.1% DMSO (vehicle) or Epac inhibitor ESI-09 (ESI) for 48 h before being harvested for RNA extraction. ESI was obtained from Selleck Chemicals (Houston, TX).

## Fatty acid measurement

Measurement was done on non-excised or exercised 16-week old wild-type,  $\text{Epac1}^{-/-}$ ,  $\text{Epac2}^{-/-}$  and  $\text{Epac1}^{-/-}; \text{Epac2}^{-/-}$  mice. For non-exercised group, chow was removed 4–6 h

prior to blood or tissues collection. Mice were trained and allowed to run on a treadmill for 31 min according to the same experimental protocol as in treadmill running test. Thirty-one min was chosen based on the initial treadmill test when none of the genotypes became exhausted but KO animals started showing difficult to catch up the pace of treadmill (as indicated by higher electric shock number and duration) (Fig. 2b). Blood were drawn and centrifuged at 2000 rpm for 10 min and plasma were collected. Tissues were snapped frozen and homogenized for FA extraction. FA contents were measured using Triglyceride Fatty Acid Quantification kit (Abcam).

## Statistical analysis

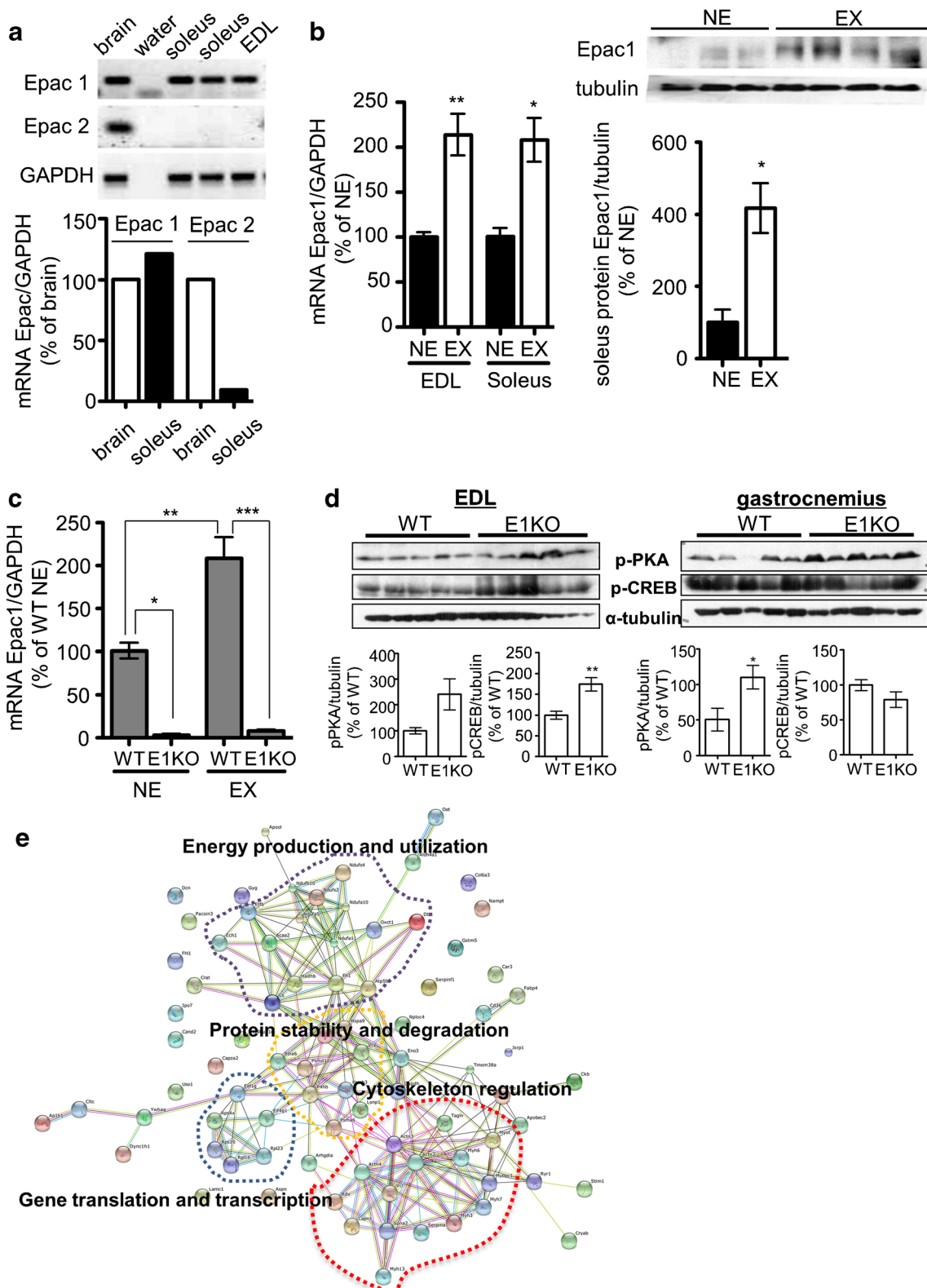
Real-time PCR quantification of mRNA level was calculated using the  $2^{-\Delta\Delta\text{Ct}}$  method. Data are presented as the mean  $\pm$  SEM of 3–5 animals and were analyzed by unpaired Student's *t* tests or one-way ANOVA followed by Dunnett *post hoc* to compare all columns against control or by Tukey's *post hoc* test to compare all pairs of columns using GraphPad Prism 5 (GraphPad Software, San Diego, CA).

## Results

### Physical activity upregulates skeletal muscle Epac1 expression and energy metabolism is altered in Epac-deficient muscle

As the first step to investigate the physiological function of Epac in skeletal muscle, the expressions of the two Epac isoforms in skeletal muscle were examined.  $\text{Epac1}$ , but not  $\text{Epac2}$ , mRNA can be easily detected in both glycolytic (extensor digitorum longus, EDL) and oxidative (soleus) types of muscles.  $\text{Epac2}$  expression in muscle was very low when compared with the brain, which expresses both Epac isoforms (Fig. 1a), confirmed by electrophoresing the PCR products to specifically amplify  $\text{Epac1}$  but no  $\text{Epac2}$  (Fig. 1a). To examine if any changes in  $\text{Epac1}$  expression in response to exercise, the expressions in non-exercised (NE) and exercised (EX)

**Fig. 1** Physical activity upregulates skeletal muscle  $\text{Epac1}$  expression and energy metabolism is altered in Epac-deficient muscle. **a** Real-time PCR analysis of  $\text{Epac1}$  and  $\text{Epac2}$  expression in EDL and soleus in resting animals and gel electrophoresis of PCR products. **b** Real-time PCR and Western blot to examine changes of  $\text{Epac1}$  mRNA and protein in non-exercised (NE) and exercised (EX) muscles. **c** Real-time PCR quantification of  $\text{Epac1}$  mRNA in wild-type and  $\text{Epac1}^{-/-}$  non-exercised and exercised soleus muscles. **d** Western blot of phospho-PKA and phospho-CREB in wild-type and  $\text{Epac1}^{-/-}$  muscles. **e** Proteins extracted from muscles of the wild-type,  $\text{Epac1}^{-/-}$ ,  $\text{Epac2}^{-/-}$  and  $\text{Epac1}^{-/-}; \text{Epac2}^{-/-}$  mice were subject to LC/MS/MS. Differentially expressed proteins were identified and represented as STRING analysis. EX: exercised; NE: non-exercised; bars represent means  $\pm$  SEM of 3–5 animals. \* $p < 0.05$ ; \*\* $p < 0.01$ ; \*\*\* $p < 0.005$



muscles were compared. Significantly elevated levels of Epac1 mRNA and protein were found in muscles collected from mice after running on treadmill (Fig. 1b). Epac1<sup>-/-</sup> mice compared with wild-type mice subjected to physical exercise

showed lack of exercise-induced Epac1 induction in Epac1<sup>-/-</sup> soleus (Fig. 1c). Interestingly, significantly elevated levels of PKA and CREB phosphorylation in exercised Epac1<sup>-/-</sup> muscle were observed (Fig. 1d). In addition, Epac1<sup>-/-</sup>, Epac2<sup>-/-</sup>

and  $\text{Epac1}^{-/-}$ ;  $\text{Epac2}^{-/-}$  mice also showed similar exercise intolerance to  $\text{Epac1}^{-/-}$  mice (data not shown). Proteomic identification and systemic analysis are powerful tools for screening the possible altered functions or pathways under specific pathophysiological conditions. In the present study, our proteomic results screened a number of possible pathways which could be altered in the soleus muscle of different types of Epac KO mice group. According to the global protein expression and functional protein interaction network analyses using the STRING program, proteins differentially expressed and altered direct (physical) and indirect (functional) pathways among wild-type,  $\text{Epac1}^{-/-}$ ,  $\text{Epac2}^{-/-}$  and  $\text{Epac1}^{-/-}$ ;  $\text{Epac2}^{-/-}$  muscles were identified (Table 1). Based on the proteomic results, we build up a hypothesis that EPAC can be the important factor for regulating skeletal muscle function and energy metabolism. The pathways involved in energy production and utilization, protein stability and degradation, gene translation and transcription, and cytoskeleton regulation were altered in  $\text{Epac1}^{-/-}$  muscles (Fig. 1e). The number of differentially expressed proteins ( $p < 0.05$ ) is 33, 43, and 44 in  $\text{Epac1}^{-/-}$ ,  $\text{Epac2}^{-/-}$  and  $\text{Epac1}^{-/-}$ ;  $\text{Epac2}^{-/-}$  respectively.  $\text{Epac1}^{-/-}$ ;  $\text{Epac2}^{-/-}$  showed to have similar to that of  $\text{Epac2}^{-/-}$  or more number to that of  $\text{Epac1}^{-/-}$  of differentially expressed proteins. The pathways that are implicated in unfolded protein response were the top pathway altered in  $\text{Epac1}^{-/-}$  muscle. Oxidative phosphorylation and mitochondrial dysfunction were among the top pathways altered in  $\text{Epac2}^{-/-}$  and  $\text{Epac1}^{-/-}$ ;  $\text{Epac2}^{-/-}$  muscles (Table 2). Moreover, lipid metabolism and energy production were among the most severely altered molecular and cellular functions in  $\text{Epac1}^{-/-}$  muscle (Table 3).

### Epac-deficient mice exhibited compromised exercise capacity

The proteomic data suggested that  $\text{Epac1}$ -deficient mice may exhibit defects energy homeostasis, which would be reflected by physical exercise performance. To address this, wild-type,  $\text{Epac1}^{-/-}$ ,  $\text{Epac2}^{-/-}$  and  $\text{Epac1}^{-/-}$ ;  $\text{Epac2}^{-/-}$  mice were subjected to graded treadmill test.  $\text{Epac1}^{-/-}$ ,  $\text{Epac2}^{-/-}$  and  $\text{Epac1}^{-/-}$ ;  $\text{Epac2}^{-/-}$  mice exhibited significantly reduced exercise capacity than wild-type mice, in terms of lower work done, shorter running distance, and shorter running time before exhaustion (Fig. 2a). Epac-deficient mice, in particular  $\text{Epac2}^{-/-}$  and  $\text{Epac1}^{-/-}$ ;  $\text{Epac2}^{-/-}$  mice, encountered higher numbers and longer duration of electric shock (Fig. 2b).

### Epac1-deficiency reduced type I muscle fiber number

Among the various muscle fiber subtypes, type I fiber is characterized by type I myosin heavy chain (MyHC) expression, high abundance of mitochondria, its high oxidative capacity, resistance to fatigue and capability to perform sustained

exercise [11]. It is possible that the compromised exercise capacity in Epac-deficient mice was a result of reduction in type I fiber number and size (atrophy). The results showed that gastrocnemius collected from  $\text{Epac1}^{-/-}$  mice contained significantly fewer type I fiber than wild-type gastrocnemius (Fig. 3a). On micrographs of higher magnification, the cross section area of type I fibers, which is a measurement of fiber size and an indication of any hypertrophy or atrophy, was measured. However, there was no significant difference between the cross-section area of wild-type and  $\text{Epac1}^{-/-}$  type I fiber (Fig. 3b). The expressions of atrophy-related genes were further examined. There was no difference in the levels of atrogen-1 and MuRF-1 mRNA between wild-type and  $\text{Epac1}^{-/-}$  gastrocnemius (Fig. 3c). Same observation was confirmed on wild-type and Epac1-deficient EDL and soleus (data not shown).

### Epac deficiency increased mitochondrial COX proteins

Epac is known to mediate resveratrol and cAMP action on mitochondrial biogenesis [28]. The impact of Epac deficiency on muscle mitochondrial content was next examined, which was measured as the ratios of mitochondrial gene DNA (COX-II or ND-1) to nuclear gene DNA ( $\beta$ -globin). Among EDL and soleus from wild-type,  $\text{Epac1}^{-/-}$ ,  $\text{Epac2}^{-/-}$  and  $\text{Epac1}^{-/-}$ ;  $\text{Epac2}^{-/-}$  mice, none of the Epac-deficient muscles contained significantly difference mitochondrial contents when compared the corresponding wild-type muscles (Fig. 4a). The expressions of several mRNA encoding proteins function in mitochondria were also quantified. Among which Tfam (mitochondrial transcription factor A), UCP-3 (mitochondrial uncoupling protein-3), and CS (citrate synthase) showed no different in muscles of different genotypes (Fig. 4b and Supplementary Fig 1). A subtle but significant increase was found in COX-IV mRNA in  $\text{Epac1}^{-/-}$  EDL when compared with wild-type EDL (Fig. 4b). The increase in COX-IV mRNA led us to examine the levels of proteins of mitochondrial complexes. At protein level, COX-IV showed a trend of increase, albeit did not reach statistical significance. Levels of CXIII subunit core 2 protein in  $\text{Epac1}^{-/-}$ ,  $\text{Epac2}^{-/-}$  and  $\text{Epac1}^{-/-}$ ;  $\text{Epac2}^{-/-}$  were higher than wild-type soleus whereas  $\text{Epac2}^{-/-}$  also contained significantly more VDAC. NDUFS4 and CXII levels were consistent among the 4 genotypes (Fig. 4c).

### Glucose uptake pathway was enhanced and PGC-1A induction was blunted in Epac1-deficient muscle

Skeletal muscle is the largest glucose sink in the body therefore plays a central role in glucose homeostasis. The impacts of Epac deficiency on glucose flux in skeletal muscle were next examined. From non-exercised mice, significantly elevated glucose transporter 4 (GLUT4) levels over wild-type

**Table 1** List and information of differentially expressed proteins

Uniprot ID	Symbol	Description	p value (ttest)		Ratio to con			
			WT vs EIKO	WT vs E2KO	WT vs DKO	EIKO/WT	E2KO/WT	DKO/WT
P28654	Dcn	Decorin; may affect the rate of fibrils formation	0.0053	0.0002	0.1041	0.2027	0.2970	0.6189
P97298	Serpinf1	Serine (or cysteine) peptidase inhibitor, clade F, member 1; neurotrophic protein; induces extensive neuronal differentiation in retinoblastoma cells. Potent inhibitor of angiogenesis. As it does not undergo the S (stressed) to R (relaxed) conformational transition characteristic of active serpins, it exhibits no serine protease inhibitory activity	0.4830	0.0002	0.1935	4.7462	18.3678	8.5449
F8VQJ3	Lamc1	Laminin, gamma 1; binding to cells via a high affinity receptor, laminin is thought to mediate the attachment, migration and organization of cells into tissues during embryonic development by interacting with other extracellular matrix components	0.0003	0.0003	0.0677	0.0100	0.0100	0.2773
P53395	Dbt	Dihydrolipoamide branched chain transacylase E2; the branched chain alpha-keto dehydrogenase complex catalyzes the overall conversion of alpha-keto acids to acyl-CoA and CO(2). It contains multiple copies of three enzymatic components: branched chain alpha-keto acid decarboxylase (E1), lipoyamide acyltransferase (E2) and lipoyamide dehydrogenase (E3)	0.0005	0.0005	0.0005	0.0100	0.0100	0.0100
P26043	Rdx	Radixin; probably plays a crucial role in the binding of the barbed end of actin filaments to the plasma membrane	0.5965	0.0009	0.0040	0.6905	0.0100	0.1013
Q9D8N0	Eef1g	Eukaryotic translation elongation factor 1 gamma; probably plays a role in anchoring the complex to other cellular components (by similarity)	0.8633	0.0022	0.9578	1.0339	0.7711	0.9817
Q9DBF1	Aldh7a1	Aldehyde dehydrogenase family 7, member A1; multifunctional enzyme mediating important protective effects. Metabolizes betaine aldehyde to betaine, an important cellular osmolyte and methyl donor. Protects cells from oxidative stress by metabolizing a number of lipid peroxidation-derived aldehydes. Involved in lysine catabolism (by similarity)	0.1751	0.0023	0.1208	0.3606	0.0000	0.3164
B9EKJ1	Spna2	Spectrin alpha 2; Fodrin, which seems to be involved in secretion, interacts with calmodulin in a calcium-dependent manner and is thus candidate for the calcium-dependent movement of the cytoskeleton at the membrane	0.2991	0.0026	0.8586	0.7734	0.0000	0.9332
COX2	Pigs2	Prostaglandin-endoperoxide synthase 2; mediates the formation of prostaglandins from arachidonate. May have a role as a major mediator of inflammation and/or a role for prostanoid signaling in activity-dependent plasticity	0.7780	0.0046	0.6071	1.1884	1.4942	1.3203
Q8K3Q4	Actn2	Actinin alpha 2; F-actin cross-linking protein which is thought to anchor actin to a variety of intracellular structures.	0.1697	0.0051	0.1983	0.5018	0.6646	0.5287
Q9CPP6	Ndufa5	This is a bundling protein (by similarity) NADH dehydrogenase (ubiquinone) 1 alpha subcomplex, 5; accessory subunit of the mitochondrial membrane respiratory chain NADH dehydrogenase (complex I), that is believed not to be involved in catalysis. Complex I functions in the transfer of electrons from NADH to the respiratory chain. The immediate electron acceptor for the enzyme is believed to be ubiquinone (by similarity)	0.2765	0.0051	0.0298	1.8737	2.2570	1.8008

Table 1 (continued)

Uniprot ID	Symbol	Description	p value (ttest)		Ratio to con			
			WT vs EIKO	WT vs E2KO	WT vs DKO	EIKO/WT	E2KO/WT	DKO/WT
Q9EPL8	Ipo7	Importin 7; functions in nuclear protein import, either by acting as autonomous nuclear transport receptor or as an adapter-like protein in association with the importin-beta subunit KPMB1. Acting autonomously is thought to serve itself as receptor for nuclear localization signals (NLS) and to promote translocation of import substrates through the nuclear pore complex (NPC) by an energy requiring, Ran-dependent mechanism. At the nucleoplasmic side of the NPC, ran binds to importin, the importin/substrate complex dissociates and importin is re-exported from the nucleus to the cytoplasm [...]	0.7477	0.0053	0.0053	1.2307	0.0100	0.0100
Q9DCS9	Ndufb10	NADH dehydrogenase (ubiquinone) 1 beta subcomplex, 10; accessory subunit of the mitochondrial membrane respiratory chain NADH dehydrogenase (complex I), that is believed not to be involved in catalysis. Complex I functions in the transfer of electrons from NADH to the respiratory chain. The immediate electron acceptor for the enzyme is believed to be ubiquinone (by similarity)	0.2708	0.0057	0.0201	0.7603	0.6223	0.6826
Q3ULT2	Actm4	Actinin alpha 4; F-actin cross-linking protein which is thought to anchor actin to a variety of intracellular structures. This is a bundling protein. Probably involved in vesicular trafficking via its association with the CART complex. The CART complex is necessary for efficient transferrin receptor recycling but not for EGFR degradation (by similarity)	0.2378	0.0065	0.1074	0.5092	0.1183	0.4553
Q3TMP8	Tmem38a	Transmembrane protein 38A; monovalent cation channel required for maintenance of rapid intracellular calcium release. May act as a potassium counter-ion channel that functions in synchronization with calcium release from intracellular stores	0.3739	0.0078	0.3739	0.0001	7.4621	0.0002
P23927	Cryab	Crystallin, alpha B; may contribute to the transparency and refractive index of the lens. Has chaperone-like activity, preventing aggregation of various proteins under a wide range of stress conditions	0.7134	0.0096	0.7502	1.6602	0.0000	1.5253
Q91WDS	Ndufs2	NADH dehydrogenase (ubiquinone) Fe-S protein 2; core subunit of the mitochondrial membrane respiratory chain NADH dehydrogenase (complex I) that is believed to belong to the minimal assembly required for catalysis. Complex I functions in the transfer of electrons from NADH to the respiratory chain. The immediate electron acceptor for the enzyme is believed to be ubiquinone (by similarity)	0.7065	0.0096	0.0237	0.8376	0.2574	0.3470
O88990	Actm3	Actinin alpha 3; F-actin cross-linking protein which is thought to anchor actin to a variety of intracellular structures. This is a bundling protein (by similarity)	0.0815	0.0100	0.0592	0.7692	0.5061	0.7299
Q99MQ4	Aspn	Asporin; binds calcium and plays a role in osteoblast-driven collagen biomineralization activity (by similarity). Critical regulator of TGF-beta in articular cartilage and plays an essential role in cartilage homeostasis and osteoarthritis (OA) pathogenesis. Negatively regulates chondrogenesis in the articular cartilage by blocking the	0.8234	0.0105	0.9315	0.8825	0.0000	1.0576

Table 1 (continued)

Uniprot ID	Symbol	Description	<i>p</i> value (ttest)		Ratio to con			
			WT vs EIKO	WT vs E2KO	WT vs DKO	EIKO/WT	E2KO/WT	DKO/WT
Q99JB8	Pascin3	TGF-beta/receptor interaction on the cell surface and inhibiting the canonical TGF-beta/Smad signal. Negatively regulates periodontal ligament (PDL) differentiation and mineralization to ensure that the PDL is not ossified and to maintain homeostasis of [...] Protein kinase C and casein kinase substrate in neurons 3; may play a role in endocytosis	0.0219	0.0114	0.1322	0.3231	0.6613	0.5043
Q99JY0	Hadhb	Hydroxyacyl-coenzyme A dehydrogenase/3-ketoacyl-coenzyme A thiolase/enoyl-coenzyme A hydratase (trifunctional protein), beta subunit	0.2081	0.0120	0.1513	0.7525	0.4798	0.5456
O35350	Capn1	Calpain 1; calcium-regulated non-lysosomal thiol-protease which catalyze limited proteolysis of substrates involved in cytoskeletal re-modeling and signal transduction	0.2056	0.0154	0.7798	1.6167	1.7027	1.1624
Q9CZU6	Cs	Citrate synthase	0.2601	0.0220	0.2016	1.6393	2.0605	1.8340
Q64727	Vcl	Vinculin; actin filament (F-actin)-binding protein involved in cell-matrix adhesion and cell-cell adhesion. Regulates cell- surface E-cadherin expression and potentiates mechanosensing by the E-cadherin complex. May also play important roles in cell morphology and locomotion (by similarity)	0.0058	0.0226	0.2637	0.7541	0.7591	0.8924
P22599	Serpina1b	Serine (or cysteine) peptidase inhibitor, clade A, member 1B; Inhibitor of serine proteases. Its primary target is elastase, but it also has a moderate affinity for plasmin and thrombin	0.5467	0.0239	0.2335	0.8602	0.4781	0.6721
Q9Z1Z0	Uso1	USO1 homolog, vesicle docking protein (yeast); general vesicular transport factor required for intercompartmental transport in the Golgi stack; it is required for transcytotic fusion and/or subsequent binding of the vesicles to the target membrane. May well act as a vesicular anchor by interacting with the target membrane and holding the vesicular and target membranes in proximity (By similarity)	0.1940	0.0239	0.2690	0.3270	0.0100	0.3865
Q3TIL8	Pdia6	Protein disulfide isomerase associated 6; may function as a chaperone that inhibits aggregation of misfolded proteins. Plays a role in platelet aggregation and activation by agonists such as convulxin, collagen, and thrombin (by similarity)	0.0394	0.0247	0.9217	2.2310	2.5461	1.1207
P04247	Mb	Myoglobin; serves as a reserve supply of oxygen and facilitates the movement of oxygen within muscles (by similarity)	0.0719	0.0258	0.0065	2.1319	2.0051	2.4634
Q04447	Ckb	Creatine kinase, brain; reversibly catalyzes the transfer of phosphate between ATP and various phosphagens (e.g., creatine phosphate). Creatine kinase isoenzymes play a central role in energy transduction in tissues with large, fluctuating energy demands, such as skeletal muscle, heart, brain, and spermatozoa	0.0017	0.0269	0.0222	9.7859	8.7288	7.1830
Q9R1P1	Psemb3	Proteasome (prosome, macropain) subunit, beta type 3; the proteasome is a multicatalytic proteinase complex which is characterized by its ability to cleave peptides with Arg, Phe, Tyr, Leu, and Glu adjacent to the leaving group at neutral or slightly basic pH. The proteasome has an ATP-dependent proteolytic activity (by similarity)	0.6706	0.0302	0.9282	1.2072	0.1729	0.9109
P38647	Hspa9		0.0043	0.0317	0.3357	0.7040	0.7071	0.8382

Table 1 (continued)

Uniprot ID	Symbol	Description	p value (ttest)		Ratio to con			
			WT vs EIKO	WT vs E2KO	WT vs DKO	E1KO/WT	E2KO/WT	DKO/WT
H7BX88	Crat	Heat shock protein 9; implicated in the control of cell proliferation and cellular aging. May also act as a chaperone Carnitine acetyltransferase; carnitine acetylase is specific for short chain fatty acids. Carnitine acetylase seems to affect the flux through the pyruvate dehydrogenase complex. It may be involved as well in the transport of acetyl-CoA into mitochondria	0.0149	0.0334	0.7886	0.5896	0.6231	0.9731
Q9R0Y5	Ak1	Adenylate kinase 1; catalyzes the reversible transfer of the terminal phosphate group between ATP and AMP. Plays an important role in cellular energy homeostasis and in adenine nucleotide metabolism (by similarity). May provide a mechanism to buffer the adenylate energy charge for sperm motility	0.1283	0.0356	0.6134	1.3588	1.6751	1.0977
Q923F9	Ndufs4	NADH dehydrogenase (ubiquinone) Fe-S protein 4; accessory subunit of the mitochondrial membrane respiratory chain NADH dehydrogenase (complex I), that is believed not to be involved in catalysis. Complex I functions in the transfer of electrons from NADH to the respiratory chain. The immediate electron acceptor for the enzyme is believed to be ubiquinone	0.0574	0.0365	0.0176	0.4855	0.4332	0.1403
P37804	Tagln	Transgelin; actin cross-linking/gelling protein (by similarity)	0.1552	0.0388	0.7498	0.4626	0.1822	0.8085
Q542H7	Fabp4	Fatty acid binding protein 4, adipocyte; lipid transport protein in adipocytes. Binds both long-chain fatty acids and retinoic acid. Delivers long-chain fatty acids and retinoic acid to their cognate receptors in the nucleus	0.0544	0.0395	0.0304	0.5848	0.4769	0.5082
Q9CR57	Rpl14	Ribosomal protein L14	0.3738	0.0408	0.1422	0.0004	28.2277	13.0004
P13541	Myh3	Myosin, heavy polypeptide 3, skeletal muscle, embryonic; muscle contraction	0.0826	0.0415	0.0213	0.8936	0.8981	0.8609
Q3MI48	Jsrp1	Junctional sarcoplasmic reticulum protein 1; involved in skeletal muscle excitation/contraction coupling (EC), probably acting as a regulator of the voltage-sensitive calcium channel CACNA1S (by similarity). EC is a physiological process whereby an electrical signal (depolarization of the plasma membrane) is converted into a chemical signal, a calcium gradient, by the opening of ryanodine receptor calcium release channels. May regulate CACNA1S membrane targeting and activity	0.4613	0.0447	0.5117	0.6958	0.6637	0.8905
Q99LC3	Ndufa10	NADH dehydrogenase (ubiquinone) 1 alpha subcomplex 10; accessory subunit of the mitochondrial membrane respiratory chain NADH dehydrogenase (complex I), that is believed not to be involved in catalysis. Complex I functions in the transfer of electrons from NADH to the respiratory chain. The immediate electron acceptor for the enzyme is believed to be ubiquinone (by similarity)	0.2866	0.0497	0.0662	33.8520	6.8276	11.2669
P16858	Gapdh	Glyceraldehyde-3-phosphate dehydrogenase	0.0968	0.0510	0.0053	1.4207	1.2691	1.5832
Q01853	Vcp	Valosin containing protein; necessary for the fragmentation of Golgi stacks during mitosis and for their reassembly after mitosis. Involved in the formation of the transitional endoplasmic reticulum (tER). The transfer of membranes from the endoplasmic reticulum to the Golgi apparatus occurs via 50–70 nm transition vesicles which derive from	0.2533	0.0523	0.0295	0.8017	0.6615	0.6099

Table 1 (continued)

Uniprot ID	Symbol	Description	p value (ttest)		Ratio to con			
			WT vs EIKO	WT vs E2KO	WT vs DKO	EIKO/WT	E2KO/WT	DKO/WT
P62702 Q80U89	Rps4x Cltc	part-rough, part-smooth transitional elements of the endoplasmic reticulum (tER). Vesicle budding from the tER is an ATP-dependent process. The ternary complex containing UFD1L, VCP, and NPLOC4 binds ubiquitinated proteins and is necessary for the e [...] Ribosomal protein S4, X-linked Clathrin, heavy polypeptide (Hc); clathrin is the major protein of the polyhedral coat of coated pits and vesicles. Two different adapter protein complexes link the clathrin lattice either to the plasma membrane or to the trans-Golgi network (by similarity)	0.0766 0.0236	0.0554 0.0562	0.0802 0.1124	0.1053 1.9383	0.0000 1.8868	0.0993 1.8676
A2AEX8	Fhl1	Four and a half LIM domains 1; may have an involvement in muscle development or hypertrophy. Isoform 2 binds to RBP-J and plays a negative regulatory role in the RBP-J-mediated transcription in mammalian systems	0.1599	0.0602	0.0314	0.6225	0.4979	0.3993
Q8CHT0	Aldh4a1	Aldehyde dehydrogenase 4 family, member A1; irreversible conversion of delta-1-pyrroline-5-carboxylate (P5C), derived either from proline or ornithine, to glutamate. This is a necessary step in the pathway interconnecting the urea and tricarboxylic acid cycles. The preferred substrate is glutamic gamma-semialdehyde, other substrates include succinic, glutaric and adipic semialdehydes (by similarity)	0.5669	0.0748	0.0437	0.8534	0.5527	0.5502
P09671	Sod2	Superoxide dismutase 2, mitochondrial; destroys superoxide anion radicals which are normally produced within the cells and which are toxic to biological systems	0.6807	0.0763	0.0205	0.8180	1.4335	1.6620
Q02566 P60670	Myh6 Nploc4	Myosin, heavy polypeptide 6, cardiac muscle, alpha; muscle contraction Nuclear protein localization 4 homolog ( <i>S. cerevisiae</i> ); the ternary complex containing UFD1L, VCP, and NPLOC4 binds ubiquitinated proteins and is necessary for the export of misfolded proteins from the ER to the cytoplasm, where they are degraded by the proteasome. The NPLOC4-UFD1L-VCP complex regulates spindle disassembly at the end of mitosis and is necessary for the formation of a closed nuclear envelope (by similarity)	0.0880 0.0016	0.0793 0.0939	0.0063 0.0016	0.8256 0.0100	0.8171 0.2947	0.7100 0.0000
Q9WV35	Apobec2	Apolipoprotein B mRNA editing enzyme, catalytic polypeptide 2; probable C to U editing enzyme whose physiological substrate is not yet known. Does not display detectable apoB mRNA editing. Has a low intrinsic cytidine deaminase activity. May play a role in the epigenetic regulation of gene expression through the process of active DNA demethylation (by similarity)	0.0147	0.1021	0.0438	4.4662	2.0083	3.2125
P63325	Rpsl0	Ribosomal protein S10; component of the 40S ribosomal subunit (by similarity)	0.1117	0.1127	0.0536	0.3977	0.3657	0.1997
Q91Z83	Myh7	Myosin, heavy polypeptide 7, cardiac muscle, beta; muscle contraction (by similarity)	0.1454	0.1148	0.0536	0.8296	0.8142	0.7694
Q3UJQ9	Oxct1	3-oxoacid CoA transferase 1; key enzyme for ketone body catabolism. Transfers the CoA moiety from succinate to acetoacetate. Formation of the enzyme-CoA intermediate proceeds via an unstable anhydride species formed between the carboxylate groups of the enzyme and substrate (by similarity)	0.0050	0.1254	0.0003	0.2986	0.8068	0.4026

Table 1 (continued)

Uniprot ID	Symbol	Description	p value (ttest)		Ratio to con			
			WT vs EIKO	WT vs E2KO	WT vs DKO	EIKO/WT	E2KO/WT	DKO/WT
P97807	Fhl1	Fumarate hydratase 1	0.0014	0.1323	0.0477	1.6332	1.3642	1.8449
P21550	Eno3	Enolase 3, beta muscle; appears to have a function in striated muscle development and regeneration	0.0825	0.1329	0.0370	0.8298	0.7898	0.7421
Q8CGK3	Lonp1	Lon peptidase 1, mitochondrial; ATP-dependent serine protease that mediates the selective degradation of misfolded, unassembled or oxidatively damaged polypeptides as well as certain short-lived regulatory proteins in the mitochondrial matrix. May also have a chaperone function in the assembly of inner membrane protein complexes. Participates in the regulation of mitochondrial gene expression and in the maintenance of the integrity of the mitochondrial genome. Binds to mitochondrial promoters and RNA in a single-stranded, site-specific, and strand-specific manner. May regulate mitocho [...]	0.0221	0.1425	0.3304	1.9810	1.7252	1.4580
Q6P6L5	Mybpc1	Myosin binding protein C, slow-type	0.0130	0.1493	0.4938	0.7354	0.8906	1.0397
P70302	Stim1	Stromal interaction molecule 1; plays a role in mediating store-operated Ca(2+) entry (SOCE), a Ca(2+) influx following depletion of intracellular Ca(2+) stores. Acts as Ca(2+) sensor in the endoplasmic reticulum via its EF-hand domain. Upon Ca(2+) depletion, translocates from the endoplasmic reticulum to the plasma membrane where it activates the Ca(2+) release-activated Ca(2+) (CRAC) channel subunit, TMEM142A/ORAI1 (By similarity)	0.0838	0.1557	0.0136	0.2348	0.3133	0.0000
P47754	Capza2	Capping protein (actin filament) muscle Z-line, alpha 2; F-actin-capping proteins bind in a Ca(2+)-independent manner to the fast growing ends of actin filaments (barbed end) thereby blocking the exchange of subunits at these ends. Unlike other capping proteins (such as gelsolin and severin), these proteins do not sever actin filaments	0.1272	0.1578	0.0241	21,591.9008	37,638.6504	43,935.9296
K3W4S6	Gyg	Glycogenin; self-glucosylates, via an inter-subunit mechanism, to form an oligosaccharide primer that serves as substrate for glycogen synthase	0.0280	0.1608	0.0050	48,326.6850	16,388.8175	89,108.0314
Q99KQ4	Nampt	Nicotinamide phosphoribosyltransferase; catalyzes the condensation of nicotinamide with 5-phosphoribosyl-1-pyrophosphate to yield nicotinamide mononucleotide, an intermediate in the biosynthesis of NAD. It is the rate limiting component in the mammalian NAD biosynthesis pathway	0.0029	0.2080	0.0029	0.0000	0.3822	0.0000
O35459	Echl	Enoyl coenzyme A hydratase 1, peroxisomal; isomerization of 3-trans,5-cis-dienoyl-CoA to 2-trans,4-trans-dienoyl-CoA (by similarity)	0.2177	0.2107	0.0340	0.5675	0.5462	0.2290
Q9DCW4	Etfb	Electron transferring flavoprotein, beta polypeptide; the electron transfer flavoprotein serves as a specific electron acceptor for several dehydrogenases, including five acyl-CoA dehydrogenases, glutaryl-CoA and sarcosine dehydrogenase. It transfers the electrons to the main mitochondrial respiratory chain via ETF-ubiquinone oxidoreductase (ETF dehydrogenase) (by similarity)	0.0493	0.2768	0.8152	0.7408	0.7526	0.9152
Q3TVN4	Ap1b1		0.6963	0.3149	0.0427	1.3089	0.4563	1.4432

Table 1 (continued)

Uniprot ID	Symbol	Description	p value (ttest)		Ratio to con				
			WT vs EIKO	WT vs E2KO	WT vs DKO	EIKO/WT	E2KO/WT	DKO/WT	
		Adaptor protein complex AP-1, beta 1 subunit; subunit of clathrin-associated adaptor protein complex 1 that plays a role in protein sorting in the late-Golgi/trans-Golgi network (TGN) and/or endosomes. The AP complexes mediate both the recruitment of clathrin to membranes and the recognition of sorting signals within the cytosolic tails of transmembrane cargo molecules							
Q9DI72	D10Hus1e	DNA segment, Chr 10, Johns Hopkins University 81 expressed	0.0486	0.3498	0.0173	0.5201	0.8333	0.2023	
Q9JHU4	Dync1h1	Dynein cytoplasmic 1 heavy chain 1; cytoplasmic dynein 1 acts as a motor for the intracellular retrograde motility of vesicles and organelles along microtubules. Dynein has ATPase activity; the force-producing power stroke is thought to occur on release of ADP	0.9134	0.3739	0.0232	1.1790	0.0001	10.2366	
Q9QUM9	PsmA6	Proteasome (prosome, macropain) subunit, alpha type 6; The proteasome is a multicatalytic proteinase complex which is characterized by its ability to cleave peptides with Arg, Phe, Tyr, Leu, and Glu adjacent to the leaving group at neutral or slightly basic pH. The proteasome has an ATP-dependent proteolytic activity	0.3739	0.3739	0.0042	29,086.7042	22,287.9444	120,896.0638	
E9Q9E1	Eif4g1	Eukaryotic translation initiation factor 4, gamma 1; component of the protein complex eIF4F, which is involved in the recognition of the mRNA cap, ATP-dependent unwinding of 5'-terminal secondary structure and recruitment of mRNA to the ribosome (by similarity)	0.0028	0.3884	0.9857	1.6649	1.3166	1.0099	
P16015	Car3	Carbonic anhydrase 3; reversible hydration of carbon dioxide	0.0098	0.4025	0.3133	1.9524	1.4068	1.2808	
Q9CZB4	ApoO1	Apolipoprotein O-like	0.6464	0.4794	0.0029	1.3548	0.5528	0.0100	
E9PWQ3	Col6a3	Collagen, type VI, alpha 3	0.0125	0.4900	0.1377	1.9042	1.3781	2.4071	
Q9D8W5	PsmD12	Proteasome (prosome, macropain) 26S subunit, non-ATPase, 12; acts as a regulatory subunit of the 26S proteasome which is involved in the ATP-dependent degradation of ubiquitinated proteins	0.0516	0.5008	0.7000	2.4795	1.4934	1.2116	
O08559	Bin1	Bridging integrator 1; may be involved in regulation of synaptic vesicle endocytosis. May act as a tumor suppressor and inhibits malignant cell transformation	0.1355	0.5048	0.0048	0.7642	1.2172	0.5043	
Q99PT1	ArhGdia	Rho GDP dissociation inhibitor (GDI) alpha; regulates the GDP/GTP exchange reaction of the Rho proteins by inhibiting the dissociation of GDP from them, and the subsequent binding of GTP to them. In glioma cells, inhibits cell migration and invasion by mediating the signals of SEMA5A and PLXNB3 that lead to inactivation of RAC1 (by similarity)	0.0463	0.5571	0.3377	0.6009	0.9045	0.7526	
P29758	Oat	Omitidine aminotransferase	0.7691	0.5642	0.0113	1.1496	1.5528	1.5694	
A81P69	Ywhag	Tyrosine 3-monooxygenase/tryptophan 5-monooxygenase activation protein, gamma polypeptide; adapter protein implicated in the regulation of a large spectrum of both general and specialized signaling pathways. Binds to a large number of partners, usually by recognition of a phosphoserine or phosphothreonine motif. Binding generally results in the modulation of the activity of the binding partner	0.4426	0.5781	0.0486	1.2994	1.2905	1.4172	
E9PZQ0	Ryr1	Ryanodine receptor 1, skeletal muscle	0.0300	0.5968	0.6100	0.8789	0.9377	0.9537	
Q08857	Cd36		0.6819	0.6188	0.0391	1.3048	1.4385	4.6144	

Table 1 (continued)

Uniprot ID	Symbol	Description	p value (ttest)		Ratio to con			
			WT vs EIKO	WT vs E2KO	WT vs DKO	EIKO/WT	E2KO/WT	DKO/WT
P62830 Q9JIF9	Rpl23 Myot	CD36 antigen; seems to have numerous potential physiological functions. Binds to collagen, thrombospondin, anionic phospholipids, and oxidized LDL. May function as a cell adhesion molecule. Directly mediates cytoadherence of <i>Plasmodium falciparum</i> parasitized erythrocytes. Binds long-chain fatty acids and may function in the transport and/or as a regulator of fatty acid transport (by similarity). Receptor for thrombospondins, THBS1 AND THBS2, mediating their angiogenic effects (by similarity) Ribosomal protein L23	0.9857 0.7410	0.7233 0.7237	0.0520 0.0010	0.9956 1.0514	0.9183 0.9052	0.2074 0.8331
Q9JKS4 P09103	Ldb3 P4hb	the Z lines in muscle cells (by similarity) LIM domain binding 3 Prolyl 4-hydroxylase, beta polypeptide; This multifunctional protein catalyzes the formation, breakage and rearrangement of disulfide bonds. At the cell surface, seems to act as a reductase that cleaves disulfide bonds of proteins attached to the cell. May therefore cause structural modifications of exofacial proteins. Inside the cell, seems to form/rearrange disulfide bonds of nascent proteins. At high concentrations, functions as a chaperone that inhibits aggregation of misfolded proteins. At low concentrations, facilitates aggregation (antichaperone activity). May be involved with [...]	0.0277 0.0479	0.7349 0.7800	0.0394 0.0449	0.8193 0.2214	0.9677 0.8480	0.7647 0.5137
P56480 Q6ZQ73	Atp5b Cand2	ATP synthase, H+ transporting mitochondrial F1 complex, beta subunit Cullin-associated and neddylation-dissociated 2 (putative); probable assembly factor of SCF (SKP1-CUL1-F-box protein) E3 ubiquitin ligase complexes that promotes the exchange of the substrate-recognition F-box subunit in SCF complexes, thereby playing a key role in the cellular repertoire of SCF complexes (by similarity)	0.1899 0.0423	0.8043 0.8174	0.0281 0.6638	1.1698 2.0329	0.9879 0.8643	1.1001 1.3914
G5E814	Ndufa11	NADH dehydrogenase (ubiquinone) 1 alpha subcomplex 11; accessory subunit of the mitochondrial membrane respiratory chain NADH dehydrogenase (complex I), that is believed not to be involved in catalysis. Complex I functions in the transfer of electrons from NADH to the respiratory chain. The immediate electron acceptor for the enzyme is believed to be ubiquinone (by similarity)	0.3955	0.8918	0.0091	3.2065	1.2296	6.8699
E9PVM7	Gstm5	Glutathione S-transferase, mu 5; conjugation of reduced glutathione to a wide number of exogenous and endogenous hydrophobic electrophiles	0.0258	0.9106	0.8327	2.3228	1.0671	1.0584
Q8BWT1	Acaa2	Acetyl-coenzyme A acyltransferase 2 (mitochondrial 3-oxoacyl-coenzyme A thiolase); abolishes BNIP3-mediated apoptosis and mitochondrial damage (by similarity)	0.0483	0.9232	0.3566	1.5885	0.9814	1.3696
B1AR69	Myh13	Myosin, heavy polypeptide 13, skeletal muscle	0.0300	0.9674	0.1954	0.7668	0.9971	0.8704

*Italic numbers indicate p values less than or equal to 0.05*

**Table 2** Top canonical pathways altered in Epac-deficient muscles

Canonical pathways	<i>p</i> value	Molecules
WT vs E1KO		
Unfolded protein response	0.003467369	HSPA9, P4HB
Creatine-phosphate biosynthesis	0.006456542	CKB
Branched chain $\alpha$ -keto acid dehydrogenase complex	0.006456542	DBT
Glycogen biosynthesis II (from UDP-D-glucose)	0.009772372	GYG1
NAD biosynthesis III	0.009772372	NAMPT
WT vs E2KO		
Oxidative phosphorylation	1.23027E-07	NDUFA10, NDUFS2, NDUFA5, MT-CO2, NDUFS4, NDUFB10
Regulation of cellular mechanics by calpain protease	1.44544E-07	VCL, CAPN1, ACTN2, ACTN4, Actn3
Mitochondrial dysfunction	1.77828E-06	NDUFA10, NDUFS2, NDUFA5, MT-CO2, NDUFS4, NDUFB10
Actin cytoskeleton signaling	6.91831E-06	MYH3, VCL, ACTN2, ACTN4, Actn3, RDX
Remodeling of epithelial adherens junctions	1.41254E-05	VCL, ACTN2, ACTN4, Actn3
WT vs DKO		
Mitochondrial dysfunction	6.60693E-08	SOD2, NDUFS2, NDUFA11, NDUFA5, ATP5B, NDUFS4, NDUFB10
Oxidative phosphorylation	1.07152E-07	NDUFS2, NDUFA11, NDUFA5, ATP5B, NDUFS4, NDUFB10
Arginine degradation I (arginase pathway)	2.63027E-05	OAT, ALDH4A1
Actin cytoskeleton signaling	9.12011E-05	MYH3, MYH7, MYH6, Actn3, RDX
Epithelial adherens junction signaling	0.000251189	MYH3, MYH7, MYH6, Actn3

were consistently found in Epac1<sup>-/-</sup>, Epac2<sup>-/-</sup> and Epac1<sup>-/-</sup>; Epac2<sup>-/-</sup> soleus (Fig. 5a). AMPK is activated by exercise to promote GLUT4-mediated glucose uptake by skeletal muscle [31]. In addition to the upregulation of GLUT4, a more profound AMPK activation was observed in Epac1<sup>-/-</sup> gastrocnemius (Fig. 5b) and EDL (data not shown) collected after exercise. The SIRT1/PGC-1 $\alpha$  (peroxisome proliferator-activated receptors (PPAR) gamma coactivator-1 $\alpha$ ) axis is a critical energy sensing pathway coordinating energy homeostasis. PGC-1 $\alpha$  is highly expressed in metabolic organs/tissues of high energy demand (like type I muscle fiber, brown adipose tissue, and heart) and is induced under conditions of increased metabolic demand like during aerobic exercise. Upregulation of SIRT1 protein was detected in non-exercised Epac KO soleus, in particular in Epac2<sup>-/-</sup> soleus (Fig. 5c). In line with this observation, a robust elevation of SIRT1 was seen in soleus collected after exercise (data not shown). The influence of Epac deficiency on PGC-1 $\alpha$  mRNA expression was then examined. Soleus isolated from resting mice of different genotypes expressed similar levels of PGC-1 $\alpha$  (Fig. 5d). PGC-1 $\alpha$  expression was markedly induced in wild-type soleus after exercise, and the induction was significantly lower in the Epac1<sup>-/-</sup> and Epac1<sup>-/-</sup>; Epac2<sup>-/-</sup> soleus (Fig. 5d). In in vitro myotube culture, Epac antagonist ESI reduced PGC-1 $\alpha$  mRNA significantly (Fig. 5e).

### Epac deficiency impaired skeletal muscle lipid metabolism

As lipid is the preferable substrate for energy production in oxidative type fiber [15, 33], the impacts of Epac deficiency on lipid metabolism were focused on oxidative type muscle. Gene expressions in wild-type and KO gastrocnemius were first compared. Transcription factors like ERR $\alpha$  and PPAR $\delta$  were consistently and significantly reduced in Epac1<sup>-/-</sup>, Epac2<sup>-/-</sup> and Epac1<sup>-/-</sup>; Epac2<sup>-/-</sup> gastrocnemius (Fig. 6a). Fabp3 and CD36 are the principal molecules facilitating skeletal muscle FA uptake, Epac1<sup>-/-</sup> gastrocnemius expressed less CD36 mRNA than wild-type whereas the levels of both Fabp3 and CD36 in Epac2<sup>-/-</sup> and Epac1<sup>-/-</sup>; Epac2<sup>-/-</sup> gastrocnemius were significantly lower than wild-type (Fig. 6b). The two genes, Cpt-1a and Cpt-2, involved in FA activation were significantly lower in the three Epac-deficient gastrocnemius (Fig. 6b). Expressions of genes participating in FA oxidation were also measured. In Epac1<sup>-/-</sup>, Epac2<sup>-/-</sup> and Epac1<sup>-/-</sup>; Epac2<sup>-/-</sup> gastrocnemius, significant reduction of Acadl, Acadvl, and Decr1 was observed, whereas expression of Acadm, HadhA, and HadhB was unchanged (Fig. 6c).

In gastrocnemius and soleus isolated from resting animals, FA contents tended to be lower in Epac1<sup>-/-</sup>, Epac2<sup>-/-</sup> and Epac1<sup>-/-</sup>; Epac2<sup>-/-</sup> muscles. Epac1<sup>-/-</sup>; Epac2<sup>-/-</sup>

**Table 3** Top molecular and cellular functions altered in Epac-deficient muscles

	<i>p</i> value	Molecules
WT vs E1KO		
Lipid metabolism	8.75E-04	ACAA2, FABP4, FH, OXCT1, CRAT, NMPT
Small molecule biochemistry	8.75E-04	ACAA2, FABP4, FH, P4HB, OXCT1, CKB, GSTM3, NMPT, APOBEC2, CLTC, CRAT
Cell-to-cell signaling and interaction	1.08E-03	DCN, VCL, ARHGDI, CLTC, LAMC1, P4HB
Cell morphology	1.31E-03	ARHGDI, VCL, LAMC1, LDB3, CLTC, CKB, NAMPT, NDUFS4, EIF4G1, RYR1, DCN
Energy production	1.44E-03	ETFB, NAMPT, RYR1, FH, P4HB
WT vs E2KO		
Cellular movement	3.69E-05	ACTN4, CAPN1, DCN, MB, SERPINA1, SERPINF1, VCL, VCP, CRYAB, TAGLN, LAMC1
Cellular assembly and organization	4.56E-05	ACTN2, ACTN4, GAPDH, LAMC1, RDX, SERPINF1, SPTAN1, VCL, USO1, AK1, NDUFS4, CRYAB, CLTC, DCN, VCP, CAPN1
Cell death and survival	1.27E-04	CAPN1, CRYAB, GAPDH, MB, SERPINF1, RDX, NDUFS4, AK1, HSPA9, DCN, SERPINA1, LAMC1, VCP
Cellular function and maintenance	2.98E-04	ACTN2, AK1, CAPN1, CKB, CLTC, CRYAB, FABP4, SERPINA1, TMEM38A, VCP, VCL, USO1, HSPA9, RDX, GAPDH, SPATAN1, ACTN4
Protein degradation	2.98E-04	CAPN1, CRYAB, GAPDH, PSMB3, SERPINA1, VCP
WT vs DKO		
Cellular compromise	3.53E-08	BIN1, MYH6, MYOT, NAMPT, STIM1, VCP, NDUFS4, RDX, SOD2, CYNC1H1
Cellular assembly and organization	1.31E-05	BIN1, FHL1, MYH6, MYH7, NDUFS4, SOD2, VCP, STIM1, GAPDH, FHL1, LDB3, RDX, CKB, YWHAG, AP1B
Cellular development	1.31E-05	BIN1, DYNC1H1, GAPDH, IPO7, MB, NAMPT, SOD2, STIM1, YWHAG, FHL1, LDB3, MYH6, MB, FABP4, CD36
Cellular growth and proliferation	1.31E-05	BIN1, DYNC1H1, GAPDH, IPO7, MB, NAMPT, SOD2, STIM1, YWHAG, FHL1, LDB3, MYH6, IPO7, FABP4, CD36
Small molecule biochemistry	1.31E-05	FH, RDX, DYNC1H1, FABP4, ATP5B, CD36, NAMPT, SOD2, VCP, MB, P4HB, OXCT1, CKB, OAT, APOBEC2

gastrocnemius and Epac2<sup>-/-</sup> and Epac1<sup>-/-</sup>; Epac2<sup>-/-</sup> soleus contained significantly less FA than wild-type (Fig. 6d and Supplementary Figure 2). Importantly, FA content in wild-type soleus dropped significantly after 31-min treadmill running, indicating utilization of FA (Fig. 6d). However, there was no reduction of FA content in all three types of KO soleus. There was no statistically significant difference and changes in heart FA content (Fig. 6d).

## Discussion

Firstly, the present study demonstrated that Epac1 is the major isoform expressing in skeletal muscle. Epac1 was induced in both oxidative and glycolytic type of muscles in response to increase metabolic demand. More importantly, Epac2 mRNA was not detected nor elevated in Epac1 KO muscle and even in exercised muscle in which Epac1 was significantly induced in wild-type animal. Importantly, in Epac1 KO EDL and gastrocnemius, there were elevated levels of PKA and the

downstream CREB activation in Epac1<sup>-/-</sup> muscle than wild-type muscle, possibly a compensatory effect on Epac1-deficiency by PKA/CREB signaling, nevertheless, Epac1<sup>-/-</sup> muscle and mice exhibited molecular and physiologic phenotypes distinct from the wild-type counterpart. This observation highlighted that Epac1 possess unique roles in skeletal muscle which cannot be compensated by PKA.

Both contractile and metabolic properties of skeletal muscle are determined by the composition of fiber types: type I (slow-twitch) fiber, type IIb (fast-twitch) fibers and intermediate types IIa and IIx. Among which, type I fiber is capable to perform sustained exercise as it contains abundant mitochondria and type I myosin heavy chain (MyHC), exhibits high oxidative capacity and is resistant to fatigue [11]. Fiber composition of skeletal muscle is dynamic and can be modulated by electric stimulation and exercise. Activation of  $\beta$ -adrenergic/cAMP signaling by clenbutol caused conversion of slow to fast type fiber/decreased type I MyHC expression [7, 35], whereas diminishing  $\beta$ -adrenergic signaling leads to a shift to oxidative fiber [9, 36]. On Epac1<sup>-/-</sup> and wild-type

**Fig. 2** Epac-deficient mice exhibited compromised exercise capacity. Wild-type Epac1<sup>+/+</sup>, Epac2<sup>-/-</sup> and Epac1<sup>-/-</sup>; Epac2<sup>-/-</sup> mice were subjected to graded treadmill test. **a** Running distance and running time before exhaustion were recorded and work done were calculated. **b** Number and time of electric shock experienced by the mice were recorded and were plotted as a function of time. Bars represent means ± SEM of 3–5 animals. \**p* < 0.05; \*\**p* < 0.01; \*\*\**p* < 0.005

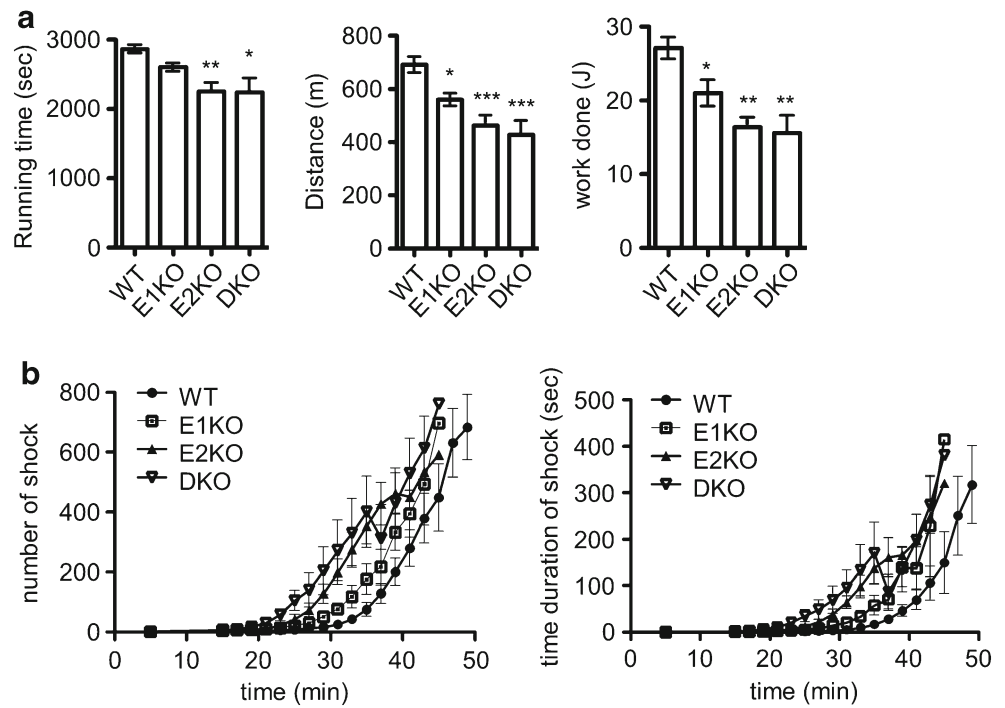


**Fig. 3** Epac1-deficiency reduced type I muscle fiber number. **a** Representative micrographs of wild-type and Epac1<sup>-/-</sup> gastrocnemius immunostained with type I myosin heavy chain antibody. **b** Micrographs of higher magnification for the quantification of cross-section area of type I fiber. **c** Real-time PCR analysis of mRNA levels of atrophy-related genes in gastrocnemius. Bars represent means ± SEM of 4–5 animals. \**p* < 0.05

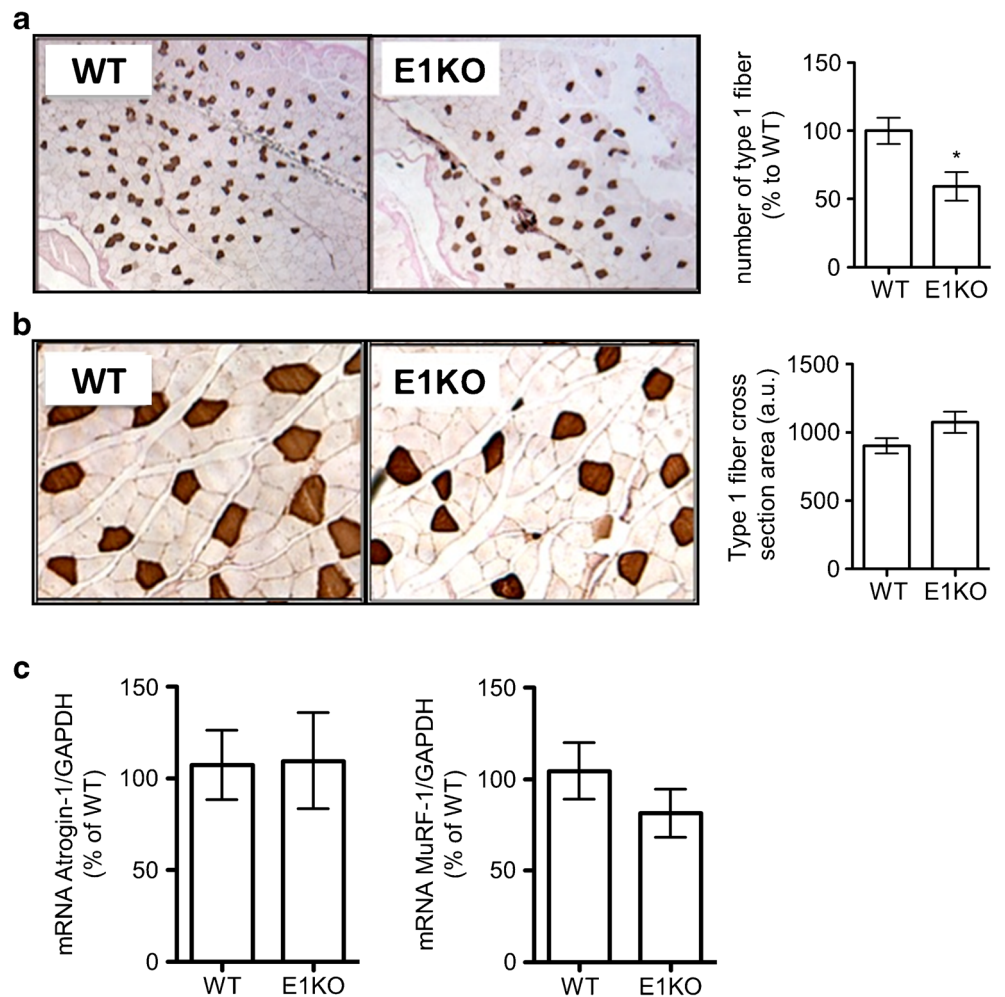
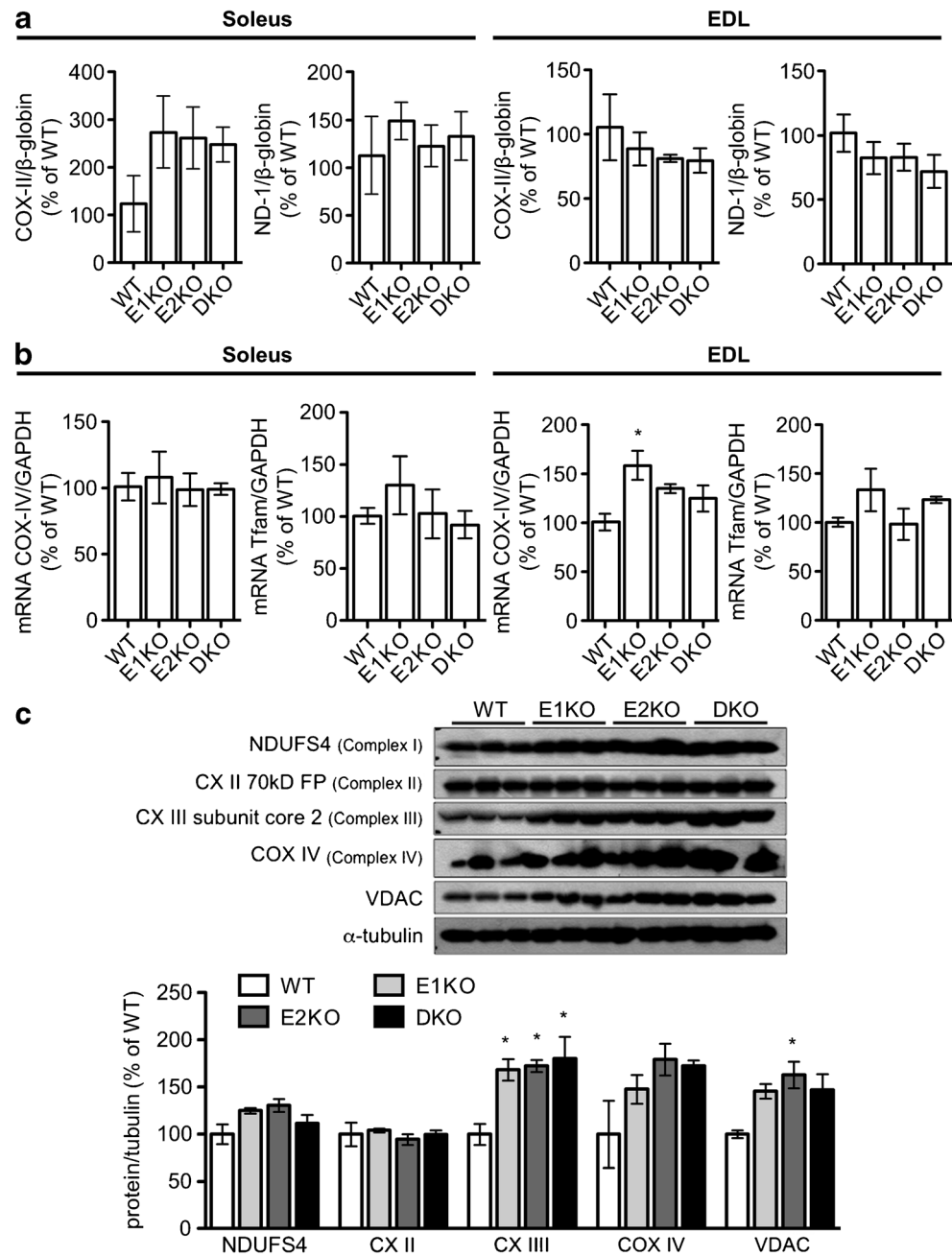


**Fig. 4** Epac deficiency increased mitochondrial COX proteins. **a** Levels of mitochondrial DNA in non-exercised soleus or EDL measured by real-time PCR and expressed as ratios to nuclear DNA. **b** Real-time PCR quantification of mRNA of mitochondrial genes and genes encoding proteins function in mitochondria in soleus or EDL. **c** Western blot of mitochondrial complex proteins in soleus. Bars represent means  $\pm$  SEM of 3 animals. \* $p < 0.05$ ; \*\* $p < 0.01$

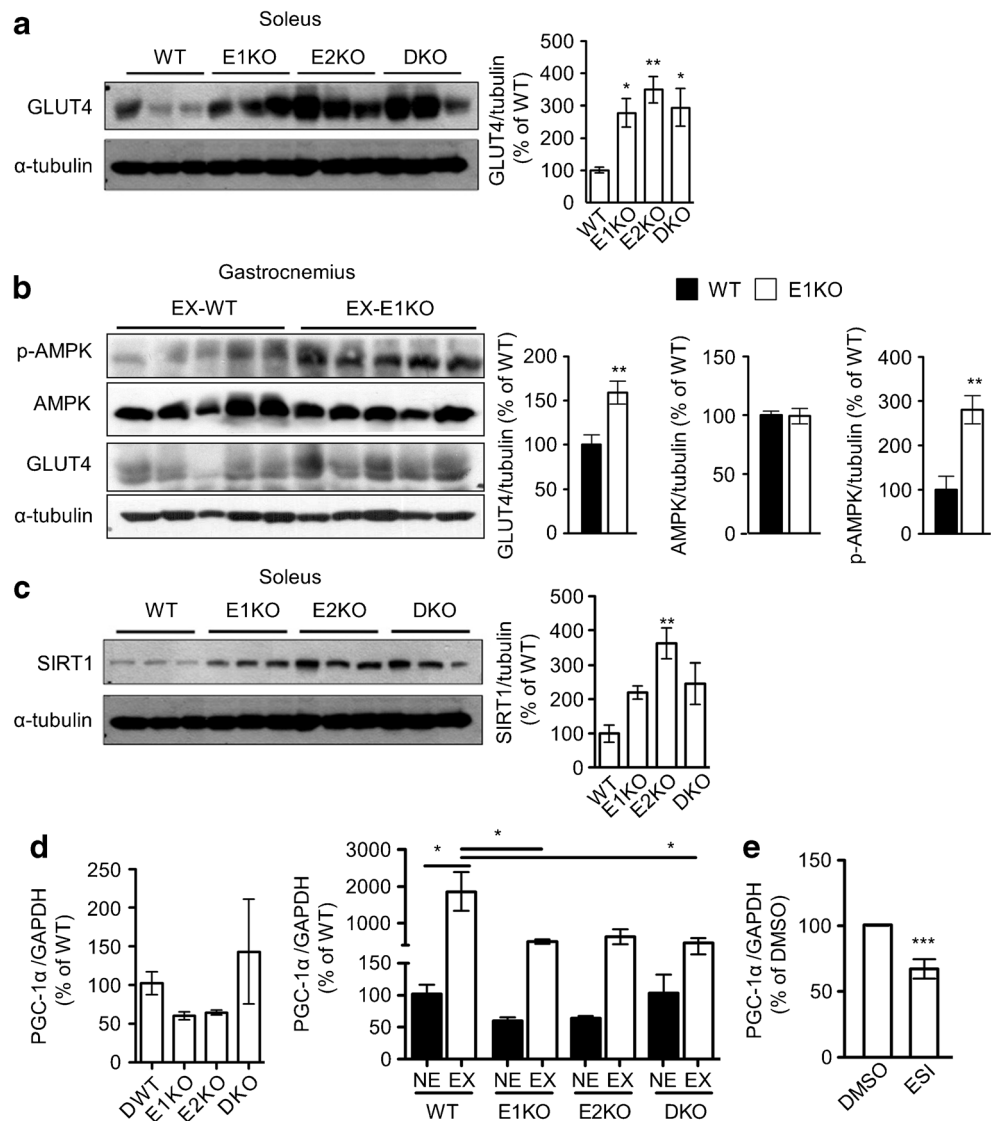


gastrocnemius, type I fiber is marked by type I MyHC immunostaining and the number of type I fiber in Epac1 KO mice muscle was significantly lower than wild-type.

Muscle hypertrophy (physiologic) and atrophy would positively and negatively impact on physical performance, respectively; however, the impact of Epac on muscle trophicity is largely unknown. Epac has been shown play a role in the development of cardiac hypertrophy [23]. Using pharmacological Epac selective agonist, Epac activation has been shown to elevate activation of AKT and Foxo3a and to mediate the anti-proteolytic effect of catecholamine in rat EDL muscle ex vivo [4]. These lines of evidence made us

hypothesized that Epac1-deficiency would lead to muscle atrophy and reduction of fiber size. Nevertheless, the cross-section area of wild-type and Epac1<sup>-/-</sup> muscle fibers was comparable, as well as the expressions of atrophy-related genes (atrogin-1 and MuRF-1). There was no consistent reduction of muscle masses in the knockout mice (data not shown). Taken together, muscle atrophy was not resulted from Epac ablation and not an underlying reason of the compromised physical performance. This discordancy with the anabolic role of Epac demonstrated [4] possibly arose from different experimental approaches. For instance, rat EDL was incubated with Epac agonist ex vivo for short time. In in vivo condition, the

**Fig. 5** Glucose uptake pathway was enhanced and PGC-1A induction was blunted in Epac1- deficient muscle. **a** Soleus collected from non-exercised wild-type, Epac1<sup>-/-</sup>, Epac2<sup>-/-</sup> and Epac1<sup>-/-</sup>; Epac2<sup>-/-</sup> mice were subjected to Western blot for detection of GLUT4. **b** GLUT4 and AMPK activation were detected in gastrocnemius collected from exercised wild-type and Epac1<sup>-/-</sup> mice by Western blot. **c** Expression of SIRT1 in soleus from non-exercised wild-type, Epac1<sup>-/-</sup>, Epac2<sup>-/-</sup> and Epac1<sup>-/-</sup>; Epac2<sup>-/-</sup> mice. **d** Real-time PCR quantification of PGC-1 $\alpha$  mRNA in soleus from mice with or without exercise. **e** PGC-1 $\alpha$  mRNA levels in myotube treated with Epac antagonist (ESI). EX: exercised; NE: non-exercised; bars represent means  $\pm$  SEM of 3–5 animals in A–D and represent means  $\pm$  SEM of 3 independent experiments in E. \* $p$  < 0.05; \*\* $p$  < 0.01; \*\*\* $p$  < 0.005



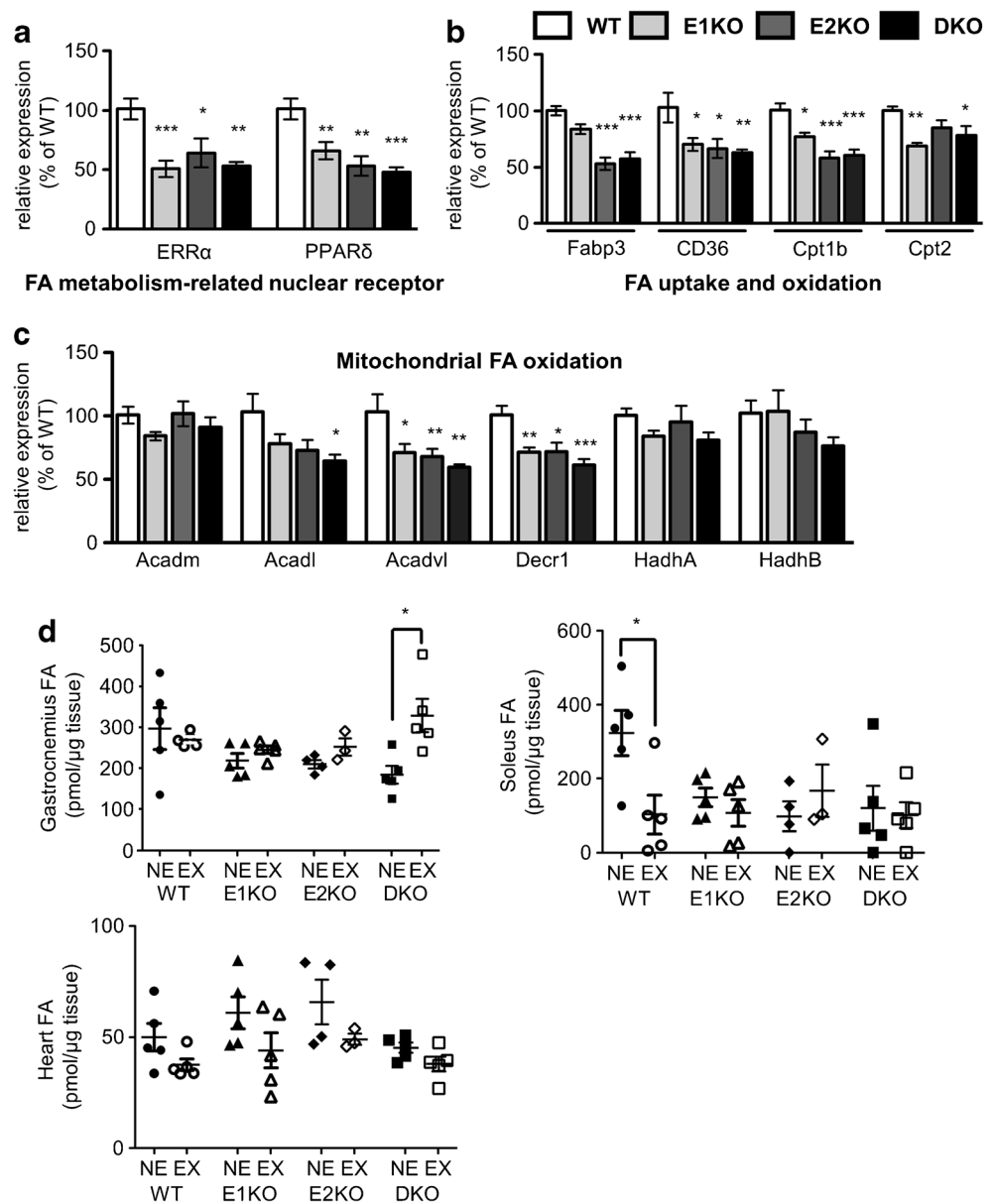
catabolic effect on skeletal muscle due to Epac deficiency may be compensated by other signaling pathways. In addition, the Epac agonist used could have off-target effects [30] especially when it is applied at high concentration [4].

During the preparation of this manuscript, a study by has been published showing that in Epac1 knockout mice,  $\beta$ -AR agonist-induced masseter muscle hypertrophy, but not type II fiber subtypes switch, was abolished [25]. However, similar phenotypes have not been observed in the Epac1<sup>-/-</sup> mice. No sign of hypertrophy or dystrophy was found in Epac1<sup>-/-</sup> muscle fibers from the Epac1 KO mice. The reason of such difference possibly arose from the different knockout strategies, strains and ages of mice used, skeletal muscle under investigation, and treatment regime.

Adrenergic/cAMP signaling pathway has well-demonstrated roles in energy sensing and energy metabolism. Evidence supporting pivotal roles of Epac in mediating cAMP signaling pathways and linking adrenergic/cAMP and

metabolic pathways is mounting [2]. Current study also shows the impact of Epac deficiency on the metabolism of the two principal substrates, glucose and fatty acid, for ATP biosynthesis in skeletal muscle. Though Epac-deficient mice ran for shorter durations and distance than wild-type mice, cellular energy sensor (AMPK activation) and glucose uptake (GLUT4 expression) were higher in Epac1<sup>-/-</sup> muscle. Moreover, elevated GLUT4 expressions were also found in Epac2<sup>-/-</sup> and Epac1<sup>-/-</sup>; Epac2<sup>-/-</sup> muscles, suggesting that elevated glucose catabolism is a common feature in Epac1<sup>-/-</sup> and Epac2<sup>-/-</sup> muscles. Previously, we have published the metabolic phenotype of epac1-deficient mice, there is no significant difference in blood glucose level between WT and Epac1<sup>-/-</sup> mice. However, Epac1<sup>-/-</sup> mice displayed the metabolic syndrome with slightly higher body weight and higher triglyceride level and more prone to develop diabetes [18]. In fact, the GLUT2 expression level was lower in epac1-deficient islets. So we were puzzled with the increased GLUT4

**Fig. 6** Epac deficiency impaired skeletal muscle lipid metabolism. **a–c** Real-time quantification of mRNA expression of nuclear receptors involved in FA metabolism (**a**) and genes involved FA uptake and activation (**b**) and mitochondrial-FA oxidation (**c**) in gastrocnemius isolated from non-exercised mice. **d** FA contents in gastrocnemius and soleus, skeletal muscle and heart in animals without exercise or after 31-min running. Data represent means  $\pm$  SEM of 3–5 animals. \* $p < 0.05$ ; \*\* $p < 0.01$ ; \*\*\* $p < 0.005$



expression level in the muscle of epac1-deficient mice. We would have to further investigate this phenotype to determine the detailed mechanism of how Epac regulate glucose transporters in various tissues.

Glucose is a preferable substrate during low to moderate intensity exercise but cannot sustain prolonged exercise and rely on FA oxidation [15, 33]. It is reasonable to speculate that the glucose catabolic pathway was more pronounced in Epac-deficient muscle as a result of compensatory response due to defective energy production process for sustainable exercise. On Epac1<sup>-/-</sup> mice, previous study has shown the mice relied on carbohydrate metabolism and therefore exhibited a higher RER [18]. A similar shift to dependence on carbohydrate catabolism and reduced physical performance was observed on Kruppel-like factor 15

knockout mice [14]. As lipids are the preferred fuel source for slow-twitch muscle and for sustained endurance exercise [15, 33], these skeletal muscle abnormalities might be due to defective lipid utilization. This prompted us to examine FA metabolism in Epac KO mice. In addition to PGC-1 $\alpha$ , levels of ERR $\alpha$  and PPAR $\delta$  were expressed at significantly lower levels in gastrocnemius from all three types of Epac deficiency mice, suggesting turning off of transcription program for FA oxidation. Recent studies suggested that EPAC1 plays a role as an upstream regulator of PGC-1 $\alpha$  and PPAR $\gamma$  or PPAR $\delta$  via C/EBP- $\beta$  signaling or CaMKK $\beta$ /Sirt1 signaling pathway [10, 17, 28]. In this context, we proposed that Epac 1 deficiency affect the upstream signal axis of PGC-1 $\alpha$  and PPAR $\delta$  and downregulated those target genes in the skeletal muscle.

Accordingly, Epac-deficient muscles contained significantly lower levels of mRNA encoding proteins implicated in various FA oxidation reactions/processes, namely FA uptake, FA activation, and FA oxidation in mitochondria. Importantly, the influence of Epac deficiency is limited and is specific to FA oxidation pathway, as there were no reductions of mitochondrial numbers and mitochondrial gene expressions; instead, dysregulation of FA oxidation gene expression affected the FA flux in muscle. Taken together, the defective FA metabolism, instead of glucose metabolism and mitochondrial functions, attributes to the compromised exercise capacity of Epac deficiency mice.

In contrast to the expression, activation, and cell autonomous nature of Epac1 demonstrated, expression studies showed a very low/no Epac2 expression in skeletal muscle; nevertheless, Epac2<sup>-/-</sup> muscles exhibited comparable phenotypes to Epac2<sup>-/-</sup> counterparts, suggesting that Epac2 functions on skeletal muscle are in a non-cell autonomous fashion. Interestingly, Epac2-deficient mice also observed some phenotypic changes in the metabolic markers similar to that of Epac1-deficient mice even though Epac1 is the major isoform of Epac expressed in the skeletal muscles. Previously, we have reported that expression of Epac2 is not altered in the Epac1 knockout brain and pancreas. However, the expression of Epac1 is lower in Epac2-deficient brain. Therefore, it is possible that the changes in the metabolic markers or phenotypes of Epac2-deficient mice in skeletal muscle may be due to this reduction of Epac1 in the Epac2-deficient mice. It is also possible that the phenotype of Epac2-deficient mice may be the result of their anxiety and depression-like phenotype of Epac2-deficient mice.

Epac2 is expressed by neurons and alters neurotransmission. Epac2 is abundantly expressed in neuronal tissues and activation of Epac by agonist enhanced neurotransmitter release in glutamatergic synapses from calyx of Held [32]. In hippocampus, Epac2 is required for the cAMP-stimulated transmitter release at the mossy fiber-CA3 synapse through maintaining the readily releasable pool at presynaptic terminal [12]. The functional roles of Epac2 at CNS and PNS levels affecting the function of neuromuscular junctions are worthy of further investigation.

In conclusion, our results demonstrate a prominent role for and underlying mechanisms of Epac in the regulation of type 1 fiber in skeletal muscle and aerobic exercise capacity. Especially, Epac 1 has a key role for transcriptional regulation of PGC-1 $\alpha$  and related FA metabolism.

**Funding information** This project is partly supported by research funding from Hong Kong Research Grant Council General Research Fund to S.K. Chung (SKC) and Small Seed Funding for Postdoctoral Fellow from Committee on Research and Conference Grants and Research Centre of Heart, Brain, Hormone and Healthy Aging, The University of Hong Kong to W.K. So and SKC; Research Grant Council Collaborative Research Fund to B.C.K Chow (SKC as co-I). Also, this work was partly supported by the National Research Foundation of Korea (NRF) and by the Ministry of Science, ICT & Future Planning of Korea (NRF-2018R1A2A3074998) to J. Han.

## Compliance with ethical standards

**Conflict of interest** The authors declare that they have no conflict of interest.

## References

1. Agbenyega ET, Morton RH, Hatton PA, Wareham AC (1995) Effect of the beta 2-adrenergic agonist clenbuterol on the growth of fast- and slow-twitch skeletal muscle of the dystrophic (C57BL/6J dy2J/dy2J) mouse. *Comp Biochem Physiol C Pharmacol Toxicol Endocrinol* 111:397–403
2. Almahariq M, Mei FC, Cheng X (2013) Cyclic AMP sensor EPAC proteins and energy homeostasis. *Trends Endocrinol Metab* 25:60–71. <https://doi.org/10.1016/j.tem.2013.10.004>
3. Baar K, Wende AR, Jones TE, Marison M, Nolte LA, Chen M, Kelly DP, Holloszy JO (2002) Adaptations of skeletal muscle to exercise: rapid increase in the transcriptional coactivator PGC-1. *FASEB J* 16:1879–1886. <https://doi.org/10.1096/fj.02-0367.com>
4. Baviera AM, Zanon NM, Navegantes LC, Kettelhut IC (2010) Involvement of cAMP/Epac/PI3K-dependent pathway in the antiproteolytic effect of epinephrine on rat skeletal muscle. *Mol Cell Endocrinol* 315:104–112. <https://doi.org/10.1016/j.mce.2009.09.028>
5. Berdeaux R, Stewart R (2012) cAMP signaling in skeletal muscle adaptation: hypertrophy, metabolism, and regeneration. *Am J Phys Endocrinol Metab* 303:E1–E17. <https://doi.org/10.1152/ajpendo.00555.2011>
6. Bos JL (2003) Epac: a new cAMP target and new avenues in cAMP research. *Nat Rev Mol Cell Biol* 4:733–738. <https://doi.org/10.1038/nrm1197>
7. Bricout VA, Serrurier BD, Bigard AX (2004) Clenbuterol treatment affects myosin heavy chain isoforms and MyoD content similarly in intact and regenerated soleus muscles. *Acta Physiol Scand* 180: 271–280. <https://doi.org/10.1046/j.0001-6772.2003.01246.x>
8. Canto C, Jiang LQ, Deshmukh AS, Matakis C, Coste A, Lagouge M, Zierath JR, Auwerx J (2010) Interdependence of AMPK and SIRT1 for metabolic adaptation to fasting and exercise in skeletal muscle. *Cell Metab* 11:213–219. <https://doi.org/10.1016/j.cmet.2010.02.006>
9. Chen M, Feng HZ, Gupta D, Kelleher J, Dickerson KE, Wang J, Hunt D, Jou W, Gavrilova O, Jin JP, Weinstein LS (2009) G(s)alpha deficiency in skeletal muscle leads to reduced muscle mass, fiber-type switching, and glucose intolerance without insulin resistance or deficiency. *Am J Phys Cell Phys* 296:C930–C940. <https://doi.org/10.1152/ajpcell.00443.2008>
10. Ding H, Bai F, Cao H, Xu J, Fang L, Wu J, Yuan Q, Zhou Y, Sun Q, He W, Dai C, Zen K, Jiang L, Yang J (2018) PDE/cAMP/Epac/C/EBP-beta signaling cascade regulates mitochondria biogenesis of tubular epithelial cells in renal fibrosis. *Antioxid Redox Signal* 29: 637–652. <https://doi.org/10.1089/ars.2017.7041>
11. Egan B, Zierath JR (2013) Exercise metabolism and the molecular regulation of skeletal muscle adaptation. *Cell Metab* 17:162–184. <https://doi.org/10.1016/j.cmet.2012.12.012>
12. Fernandes HB, Riordan S, Nomura T, Remmers CL, Kraniotis S, Marshall JJ, Kukreja L, Vassar R, Contractor A (2015) Epac2 mediates cAMP-dependent potentiation of neurotransmission in the hippocampus. *J Neurosci* 35:6544–6553. <https://doi.org/10.1523/JNEUROSCI.0314-14.2015>
13. Frey N, Frank D, Lippl S, Kuhn C, Kogler H, Barrientos T, Rohr C, Will R, Muller OJ, Weiler H, Bassel-Duby R, Katus HA, Olson EN (2008) Calcyclin-2 deficiency increases exercise capacity in mice

- through calcineurin/NFAT activation. *J Clin Invest* 118:3598–3608. <https://doi.org/10.1172/JCI36277>
14. Haldar SM, Jeyaraj D, Anand P, Zhu H, Lu Y, Prosdocimo DA, Eapen B, Kawanami D, Okutsu M, Brotto L, Fujioka H, Kerner J, Rosca MG, McGuinness OP, Snow RJ, Russell AP, Gerber AN, Bai X, Yan Z, Nosek TM, Brotto M, Hoppel CL, Jain MK (2012) Kruppel-like factor 15 regulates skeletal muscle lipid flux and exercise adaptation. *Proc Natl Acad Sci U S A* 109:6739–6744. <https://doi.org/10.1073/pnas.1121060109>
  15. Horowitz JF, Klein S (2000) Lipid metabolism during endurance exercise. *Am J Clin Nutr* 72:558S–563S
  16. Jessen N, Sundelin EI, Moller AB (2014) AMP kinase in exercise adaptation of skeletal muscle. *Drug Discov Today* 19:999–1002. <https://doi.org/10.1016/j.drudis.2014.03.009>
  17. Jia B, Madsen L, Petersen RK, Techer N, Kopperud R, Ma T, Doskeland SO, Ailhaud G, Wang J, Amri EZ, Kristiansen K (2012) Activation of protein kinase A and exchange protein directly activated by cAMP promotes adipocyte differentiation of human mesenchymal stem cells. *PLoS One* 7:e34114. <https://doi.org/10.1371/journal.pone.0034114>
  18. Kai AK, Lam AK, Chen Y, Tai AC, Zhang X, Lai AK, Yeung PK, Tam S, Wang J, Lam KS, Vanhoutte PM, Bos JL, Chung SS, Xu A, Chung SK (2013) Exchange protein activated by cAMP 1 (Epac1)-deficient mice develop beta-cell dysfunction and metabolic syndrome. *FASEB J* 27:4122–4135. <https://doi.org/10.1096/fj.13-230433>
  19. Kim HK, Kim YK, Song IS, Lee SR, Jeong SH, Kim MH, Seo DY, Kim N, Rhee BD, Ko KS, Tark KC, Park CG, Cho JY, Han J (2012) Human giant congenital melanocytic nevus exhibits potential proteomic alterations leading to melanotumorigenesis. *Proteome Sci* 10:50. <https://doi.org/10.1186/1477-5956-10-50>
  20. Kramer A, Green J, Pollard J Jr, Tugendreich S (2014) Causal analysis approaches in ingenuity pathway analysis. *Bioinformatics* 30:523–530. <https://doi.org/10.1093/bioinformatics/btt703>
  21. Lynch GS, Ryall JG (2008) Role of beta-adrenoceptor signaling in skeletal muscle: implications for muscle wasting and disease. *Physiol Rev* 88:729–767. <https://doi.org/10.1152/physrev.00028.2007>
  22. Maxwell AJ, Ho HV, Le CQ, Lin PS, Bernstein D, Cooke JP (2001). L-arginine enhances aerobic exercise capacity in association with augmented nitric oxide production. *J Appl Physiol* (1985) 90:933–938
  23. Metrich M, Lucas A, Gastineau M, Samuel JL, Heymes C, Morel E, Lezoualc'h F (2008) Epac mediates beta-adrenergic receptor-induced cardiomyocyte hypertrophy. *Circ Res* 102:959–965. <https://doi.org/10.1161/CIRCRESAHA.107.164947>
  24. Narayanasamy A, Ahn JM, Sung HJ, Kong DH, Ha KS, Lee SY, Cho JY (2011) Fucosylated glycoproteomic approach to identify a complement component 9 associated with squamous cell lung cancer (SQLC). *J Proteome* 74:2948–2958. <https://doi.org/10.1016/j.jprot.2011.07.019>
  25. Ohnuki Y, Umeki D, Mototani Y, Jin H, Cai W, Shiozawa K, Suita K, Saeki Y, Fujita T, Ishikawa Y, Okumura S (2014) Role of cyclic AMP sensor Epac1 in masseter muscle hypertrophy and myosin heavy chain transition induced by beta2-adrenoceptor stimulation. *J Physiol* 592:5461–5475. <https://doi.org/10.1113/jphysiol.2014.282996>
  26. O'Neill HM (2013) AMPK and exercise: glucose uptake and insulin sensitivity. *Diabetes Metab J* 37:1–21. <https://doi.org/10.4093/dmj.2013.37.1.1>
  27. Park HJ, Kim BG, Lee SJ, Heo SH, Kim JY, Kwon TH, Lee EB, Ryoo HM, Cho JY (2008) Proteomic profiling of endothelial cells in human lung cancer. *J Proteome Res* 7:1138–1150. <https://doi.org/10.1021/pr7007237>
  28. Park SJ, Ahmad F, Philp A, Baar K, Williams T, Luo H, Ke H, Rehmann H, Taussig R, Brown AL, Kim MK, Beaven MA, Burgin AB, Manganiello V, Chung JH (2012) Resveratrol ameliorates aging-related metabolic phenotypes by inhibiting cAMP phosphodiesterases. *Cell* 148:421–433. <https://doi.org/10.1016/j.cell.2012.01.017>
  29. Pederson BA, Cope CR, Irimia JM, Schroeder JM, Thurberg BL, Depaoli-Roach AA, Roach PJ (2005) Mice with elevated muscle glycogen stores do not have improved exercise performance. *Biochem Biophys Res Commun* 331:491–496. <https://doi.org/10.1016/j.bbrc.2005.03.206>
  30. Poppe H, Rybalkin SD, Rehmann H, Hinds TR, Tang XB, Christensen AE, Schwede F, Genieser HG, Bos JL, Doskeland SO, Beavo JA, Butt E (2008) Cyclic nucleotide analogs as probes of signaling pathways. *Nat Methods* 5:277–278. <https://doi.org/10.1038/nmeth0408-277>
  31. Richter EA, Hargreaves M (2013) Exercise, GLUT4, and skeletal muscle glucose uptake. *Physiol Rev* 93:993–1017. <https://doi.org/10.1152/physrev.00038.2012>
  32. Sakaba T, Neher E (2001) Preferential potentiation of fast-releasing synaptic vesicles by cAMP at the calyx of Held. *Proc Natl Acad Sci U S A* 98:331–336. <https://doi.org/10.1073/pnas.021541098>
  33. Shaw CS, Clark J, Wagenmakers AJ (2010) The effect of exercise and nutrition on intramuscular fat metabolism and insulin sensitivity. *Annu Rev Nutr* 30:13–34. <https://doi.org/10.1146/annurev.nutr.012809.104817>
  34. Szklarczyk D, Franceschini A, Wyder S, Forslund K, Heller D, Huerta-Cepas J, Simonovic M, Roth A, Santos A, Tsafou KP, Kuhn M, Bork P, Jensen LJ, von Mering C (2015) STRING v10: protein-protein interaction networks, integrated over the tree of life. *Nucleic Acids Res* 43:D447–D452. <https://doi.org/10.1093/nar/gku1003>
  35. van Mil HG, Kerkhof CJ, Siegenbeek van Heukelom J (1995) Modulation of the isoprenaline-induced membrane hyperpolarization of mouse skeletal muscle cells. *Br J Pharmacol* 116:2881–2888
  36. Voltarelli VA, Bacurau AV, Bechara LR, Bueno CR Jr, Bozi LH, Mattos KC, Salemi VM, Brum PC (2012) Lack of beta2-AR improves exercise capacity and skeletal muscle oxidative phenotype in mice. *Scand J Med Sci Sports* 22:e125–e132. <https://doi.org/10.1111/j.1600-0838.2012.01519.x>
  37. Zhou L, Ma SL, Yeung PK, Wong YH, Tsim KW, So KF, Lam LC, Chung SK (2016) Anxiety and depression with neurogenesis defects in exchange protein directly activated by cAMP 2-deficient mice are ameliorated by a selective serotonin reuptake inhibitor, Prozac. *Transl Psychiatry* 6:e881. <https://doi.org/10.1038/tp.2016.129>

**Publisher's note** Springer Nature remains neutral with regard to jurisdictional claims in published maps and institutional affiliations.